SECTION IV

NON-TRADITIONAL DESALINATION PROCESSES

G.P. Narayan and J.H. Lienhard V. Humidification dehumidification desalination. In J. Kucera, editor, Desalination: Water from Water, Chapter 9, pages 425–472. Wiley-Scrivener, Salem, MA, 2014.
ISBN 9781118208526.

9

Humidification Dehumidification Desalination

G. Prakash Narayan and John H. Lienhard V

Rohsenhow Kendall Heat Transfer Laboratory, Massachusetts Institute of Technology, Cambridge, MA 02139-4307 USA.

Abstract

Humidification-dehumidification (HDH) desalination involves vaporizing water from a saline liquid stream into a carrier gas stream and then condensing the vapor to form purified water. This chapter describes various forms of the HDH cycle, with analysis of the energy consumption of various realizations of the process. Bubble column dehumidifiers are described in detail.

Keywords: Humidification-dehumidification desalination, Carrier gas extraction, Bubble column dehumidifier, Thermodynamic balancing, Mass injection and extraction, Effectiveness, Gained-output-ratio, Enthalpy pinch

9.1 Introduction

More than a billion people lack access to safe drinking water worldwide [1]. A large majority of these people live in low income communities. The United Nations acknowledges this fact in its millennium development goals [2] by highlighting the critical need for impoverished and developing regions of the world to achieve self-sustenance in potable water supply. Figure 9.1 further

Jane Kucera (ed.) Desalination, (427–472) 2014 © Scrivener Publishing LLC

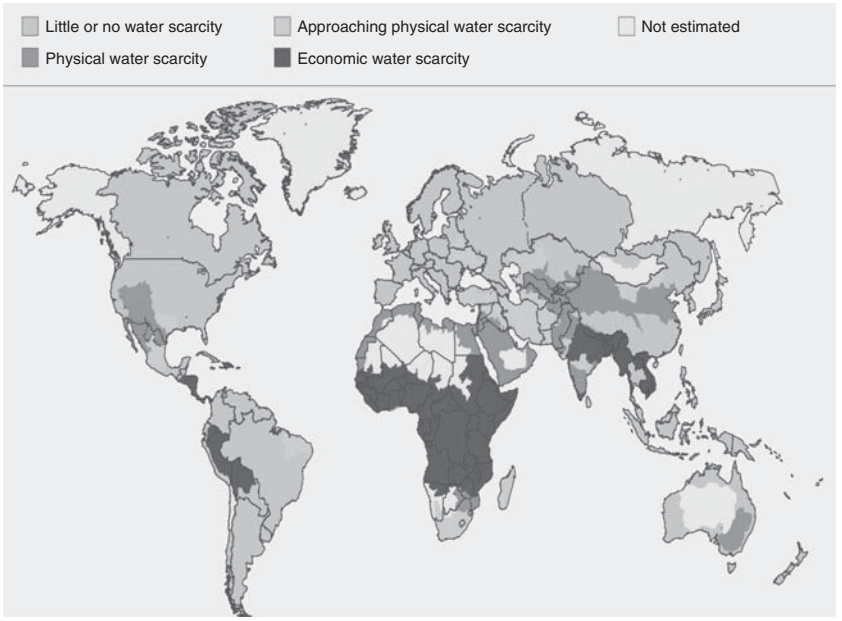

Figure 9.1 World map showing areas of physical and economic water scarcity [4].

illustrates how intense water scarcity exists mainly in the developing parts of the world[1]. For example, in India alone, 200,000 villages (and several peri-urban communities) lack access to safe potable water [3]. There is a clear need to help create a sustainable solution to the rural water problem in order to solve the global water crisis.

Most of the villages lacking safe drinking water are small communities with a population between 1,000 and 10,000 people. Thus, the minimum water needs (for drinking and cooking) for each one of those communities is between 10 and 100 cubic meter of pure water per day (at a consumption rate of 10 liters per person

[1] Often, lack of a potable water supply to the general population (or water scarcity) is misunderstood as absence of freshwater in a community. This is only one of the forms of water scarcity known as physical water scarcity. There is also scarcity in areas where there is plenty of rainfall and/or freshwater. This is primarily because of the lack of infrastructure to purify and transport the fresh water from aquifers or water bodies like lakes and rivers to the people who need it. This is termed as economic water scarcity.

per day). Systems that produce such amounts of pure water are relatively small-scale compared to conventional water treatment systems (for example, most existing state-of-the-art desalination systems are of the order of 100,000 to 1 million cubic meters per day [5]).

Any potential small-scale solution to the problem needs to be both implementable and scalable. For the solution to be implementable, it has to be cost effective and resource-frugal. Currently, the price of safe drinking water (in the rare case when it is available) in these low income communities is very high relative to the cost of centrally distributed municipal drinking water in nearby "developed" regions. For example, in some parts of rural India the cost of water is up to $\$10/m^3$ which is roughly 40 times the cost of municipal drinking water available a few miles away in a nearby city [6]. Furthermore, in many villages, resources including skilled labor, a continuous energy supply, and raw materials are not readily available. The solution should, hence, be implementable within these constraints too.

An implementable solution is truly worthwhile only if it is scalable and can reach a large number of people (say, a million or more). For such scalability, the solution should be able to handle an array of contaminants in the water to be treated. In India alone, the contaminants range from high fluoride content to bacterial contamination to water being very brackish. Sixty-six million people have been reported to be consuming water with elevated levels of fluoride in India [7]. Most of these people live in the states of Rajasthan and Gujarat where fluoride contents reach up to 11 mg/L. Some districts in Assam Orissa have very high iron content in water (1 to 10 mg/L - red water) and some in Rajasthan, Uttar Pradesh and Bihar have yellow water (>1 mg/L of iron) [8]. Certain places in Haryana, Gujarat, and Andhra Pradesh were also found to have dangerously high levels of mercury. The problems associated with high levels of arsenic in ground water (in West Bengal) are well documented [9]. At least 300,000 people are affected by drinking water with arsenic above the permissible limit of 0.05 mg/L in this region. In parts of coastal Tamil Nadu, because of seawater intrusion, there is the problem of high salinity in ground water supplies (as high as 10,000 ppm in some cases) [10]. These problems are almost exclusively limited to rural and peri-urban communities. In all, almost one in three of the 600,000

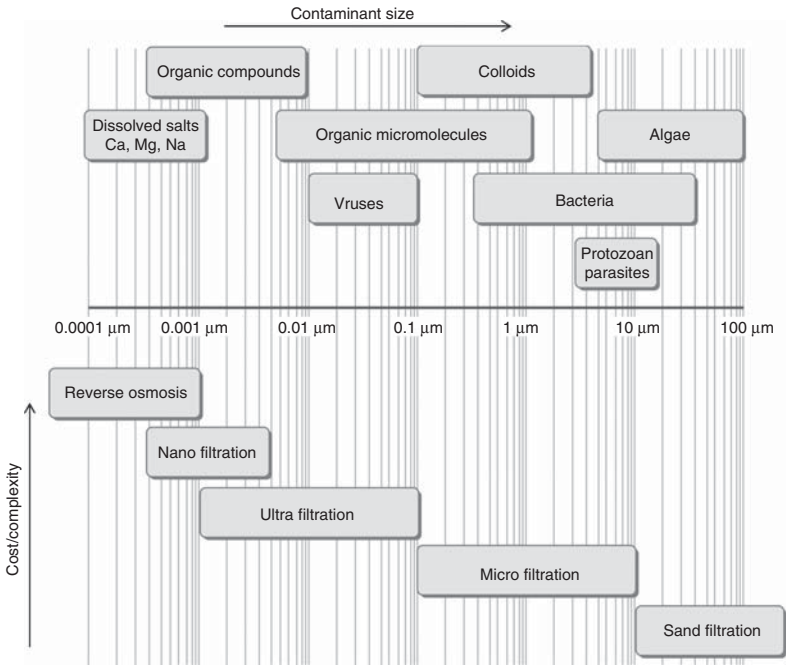

Figure 9.2 Illustration of various membrane technologies and the various contaminants they remove (Figure by MIT OpenCourseWare; data source: A. Twort et al. [11]).

Indian villages face problems of brackish or contaminated water and scarcity of fresh water. The Indian example is typical in that most developing and under-developed nations face similar water problems.

Desalination technologies can remove all contaminants including almost all dissolved ions, micro organisms and so on. For example, as illustrated in Fig. 9. 2, reverse osmosis removes even the smallest contaminants (albeit at a higher cost and complexity compared to other water treatment techniques shown in figure). Furthermore, thermal desalination technologies (MSF, MED, HDH and so on) are commonly known to remove all contaminants (producing what is in principle de-ionized water). The challenges in implementing these technologies are, however, to make them low cost ($< \$5/m^3$), to provide them at a community-scale (10–100 m^3/day), and, relatively maintenance-free (or at least maintable by non-technical laborers). Humidification dehumidification desalination offers a small-scale desalination technology which can meet these challenges.

9.1.1 Humidification Dehumidification (HDH) Desalination

Nature uses air as a carrier gas to desalinate seawater by means of the rain cycle. In the rain cycle, seawater gets heated (by solar irradiation) and evaporates into the air above to humidify it. Then the humidified air rises and forms clouds. Eventually, the clouds 'dehumidify' as rain and that which falls over land can be collected for human consumption. The man-made version of this cycle is called the humidification-dehumidification desalination (HDH) cycle. The simplest form of the HDH cycle is illustrated in Figure 9.3. The cycle consists of three subsystems: (a) an air and/or a brine heater (only a brine heater is shown in the figure), which can use various sources of energy like solar, thermal, geothermal or combinations of these; (b) the humidifier or evaporator; and (c) the dehumidifier or condenser.

The HDH cycle has received some attention in recent years and many researchers have investigated the intricacies of this technology. It should be noted here that the predecessor technology of the HDH cycle is the simple solar still. Several researchers [12–14] have reviewed the numerous works on the solar still. It is important to understand the demerits of the solar still concept.

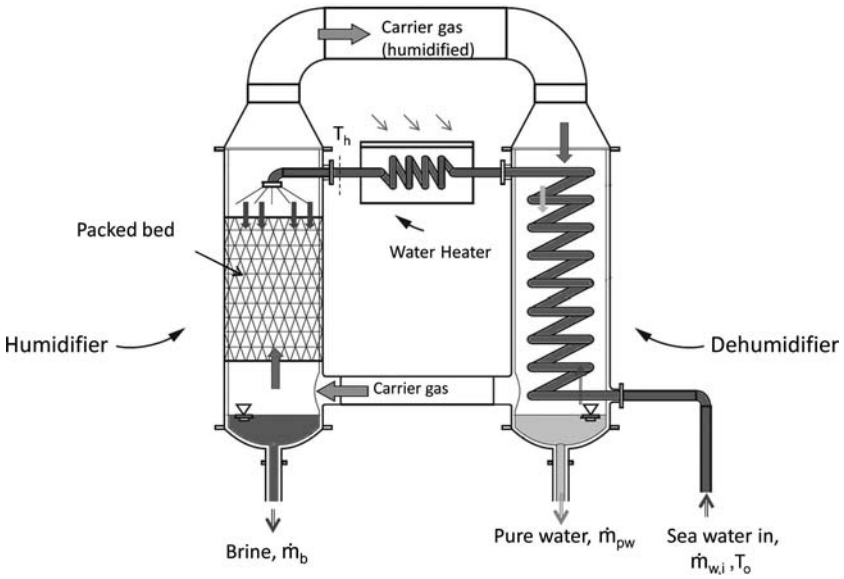

Figure 9.3 Simplest embodiment of HDH process [17].

The most prohibitive drawback of a solar still is its low efficiency (Gained-output-ratio, or GOR[2], less than 0.5) which is primarily the result of the immediate loss of the latent heat of condensation through the glass cover of the still. Some designs recover and reuse the heat of condensation, increasing the efficiency of the still. These designs (called multi-effect stills) achieve some increase in the efficiency of the still, but the overall performance is still relatively low. The main drawback of the solar still is that the various functional processes (solar absorption, evaporation, condensation, and heat recovery) all occur within a single component. By separating these functions into distinct components, thermal inefficiencies may be reduced and overall performance improved. This separation of functions is the essential characteristic of the HDH system. For example, the recovery of the latent heat of condensation, in the HDH process, is effected in a separate heat exchanger (the dehumidifier) wherein the seawater, for example, can be preheated. The module for heat input (like a solar collector) can be optimized almost independently of the humidification or dehumidification component. The HDH process, thus, promises higher productivity due to the separation of the basic processes.

HDH systems are ideal for application in small-scale systems. They have no parts which require extensive capital cost and maintenance like membranes or high temperature steam lines. There is also no barrier to applying HDH for varied and difficult feedwater qualities.

HDH systems may be classified under three broad categories. One is based on the form of energy used such as solar, thermal, geothermal, or hybrid systems. This classification brings out a promising merit of the HDH concept: the promise of water production by use of low grade energy, especially from sources of industrial waste heat or from renewable resources like solar energy or biomass.

The second classification of HDH processes is based on the cycle configuration (Figure 9.4). As the name suggests, a closed-water open-air (CWOA) cycle is one in which ambient air is taken into the humidifier where it is heated and humidified and sent to the dehumidifier where it is partially dehumidified and let out in an open cycle as opposed to a closed air cycle wherein the air is circulated in

[2] See Sec. 9.1.2 for definition of GOR.

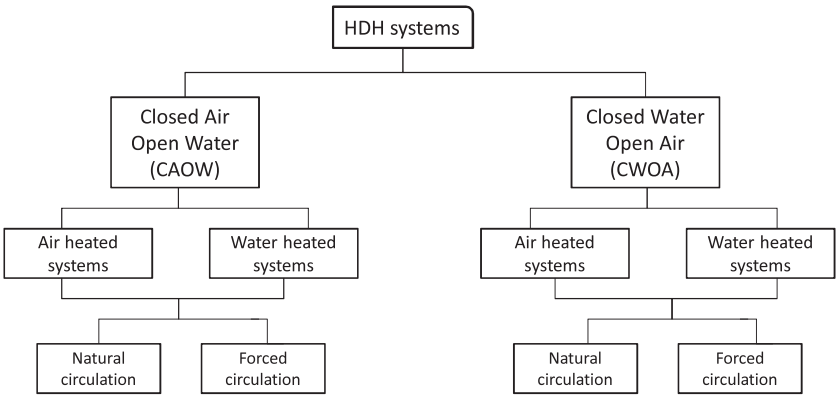

Figure 9.4 Classification of HDH systems based on cycle configurations [15].

a closed loop between the humidifier and the dehumidifier. In this cycle, the brine is recirculated until a desirable recovery is attained. The air in these systems can be circulated by either natural convection or mechanical blowers and feedwater is typically circulated by a pump. It is of pivotal importance to understand the relative technical advantages of each of these cycles and choose the configuration that is best in terms of efficiency and cost of water production.

The third classification of the HDH systems is based on the type of heating used - water or air heating systems. The performance of the system depends greatly on which fluid is heated.

9.1.2 Review of Systems in Literature

As a first step for understanding different works in literature the following performance parameters are defined.

1. Gained-Output-Ratio (GOR): is the ratio of the latent heat of evaporation of the water produced to the net heat input to the cycle.

$$\mathrm{GOR} \equiv \frac{\dot{m}_{pw} \cdot h_{fg}}{\dot{Q}_{in}} \tag{9.1}$$

This parameter is, essentially, the effectiveness of water production, which is an index of the amount of the heat recovery affected in the system. This is the primary performance parameter of interest in HDH (and in thermal desalination, in general) and is very similar to the performance ratio (PR) defined for MED and MSF systems. For

steam-driven desalination systems (like in most state-of-the-art MSF and MED systems), PR is approximately equal to GOR:

$$\mathrm{GOR} = \frac{\dot{m}_{pw} \cdot h_{fg}}{\dot{m}_s \cdot \Delta h_s} \tag{9.2}$$

$$\approx \underbrace{\frac{\dot{m}_{pw}}{\dot{m}_s}}_{\mathrm{PR}} \tag{9.3}$$

It is worthwhile to note that GOR is also defined as the ratio of the latent heat (h_{fg}) to the specific thermal energy consumption. The latent heat in the equations above is calculated at the average partial pressure of water vapor (in the moist air mixture) in the dehumidifier.

2. Recovery ratio (RR): is the ratio of the amount of water produced per kg of feed. This parameter is also called the extraction efficiency [16]. This is, generally, found to be around 5% for the HDH system in single pass and can be increased to higher values (up to 90% depending on feed salinity) by brine recirculation.

$$\mathrm{RR} \equiv \frac{\dot{m}_{pw}}{\dot{m}_w} \tag{9.4}$$

The literature has been reviewed in detail previously by the present authors [15] and the review was also updated recently [17]. Based on this review, we can benchmark the key performance metrics of existing HDH systems: (1) the cost of water production; (2) the heat and mass transfer rates in the dehumidifier; and (3) the system energy efficiency (GOR).

The total cost of water production in HDH systems is mostly a sum of the energy cost (captured by the GOR of the system) and the capital cost. A large fraction of the capital investment in typical HDH systems is the dehumidifier cost[3]. This is driven by the low heat and mass transfer rates common in such devices. It has been reported that the 'equivalent' heat transfer coefficient in the dehumidifier is between 1 and 100 W/m^{2}K [18, 19]. This is two orders of magnitude lower than for pure vapor condensers.

[3] The HDH system has relatively minimal maintenance requirements.

Using the data given in various papers, GOR for the reported systems was calculated. It was found that the maximum GOR among existing HDH systems was about 3. Figure 9.5 illustrates the GOR of a few of the studies. The GOR varied between 1.2 to 3. These values of GOR translate into energy consumption rates from 215 kWh_{th}/m^3 to 550 kWh_{th}/m^3. The low value of GOR achieved by Ben Bacha et al. [20] was because they did not recover the latent heat of condensation. Instead, they used separate cooling water from a well to dehumidify the air. Lack of a systematic understanding of the thermal design of HDH systems, which can help to optimize performance, is the reason behind such inefficient designs. The higher value of GOR achieved by Müller-Hölst et al. [21] was because of higher heat recovery. These results tell us the importance of maximizing heat recovery in minimizing the energy consumption and the operating and capital cost of HDH systems. It is also to be noted that the GOR fluctuated between 3 to 4.5 in Müller-Hölst's system because of the inability of that system to independently control the air flow under the natural convection design that was applied. It is, therefore, desirable to develop forced convection based systems which have a sustainable peak performance.

Based on a simple thermodynamic calculation, the GOR of a thermodynamically reversible HDH system can be evaluated to be 122.5 for typical boundary conditions [22]. When compared to a GOR of 3 for existing systems, the reversible GOR of 122.5 shows that there is significant potential for improvement to existing HDH

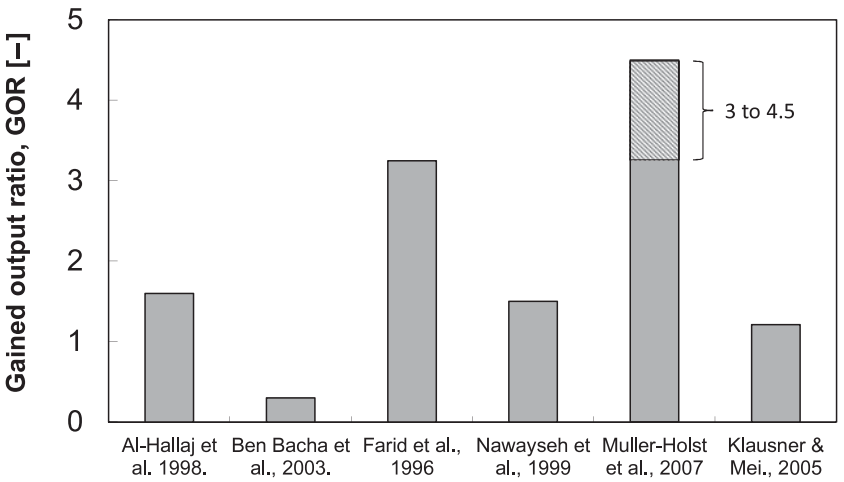

Figure 9.5 Performance of the older HDH systems in the literature [17].

systems in terms of reducing thermodynamic losses. This observation gives ample motivation to study the thermal design of these systems in detail.

A few studies in literature actually report the overall cost of water production in a HDH system [21, 23, 24]. This cost is found to be about $30 per cubic meter of water produced, which is very high. More recent work, which we describe in subsequent sections, has reduced the cost to affordable levels (< $5 per cubic meter).

9.2 Thermal Design

When finite time thermodynamics is used to optimize the energy efficiency of thermal systems, the optimal design is one which produces the minimum entropy within the constraints of the problem (such as fixed size or cost). In this section, we apply this well-established principle to the thermal design of combined heat and mass exchange devices (dehumidifiers, and humidifiers) for improving the energy efficiency of HDH desalination systems.

The theoretical framework for design of heat and mass exchange (HME) devices for implementation in the HDH system has been developed in a series of recent papers [22, 25–31]. The linchpin in this theoretical work is the definition of a novel parameter known as the 'modified heat capacity rate ratio' (HCR). A brief summary of the definition of this parameter and its significance to thermal design of HME devices and the HDH system is given below.

Modified heat capacity rate ratio

In the limit of infinite heat transfer area, the entropy generation rate in a regular heat exchanger will be entirely due to what is known as thermal imbalance. This is associated with conditions for which the heat capacity rate of the streams exchanging heat are not equal [32]. In other words, a heat exchanger (with constant heat capacity for the fluid streams) is said to be thermally 'balanced' at a heat capacity rate ratio of one. This concept of thermodynamic balancing, very well known for heat exchangers, was previously extended by the present authors to HME devices [25].

In order to define a thermally 'balanced' state in HME devices, a modified heat capacity rate ratio (HCR) for combined heat and

mass exchangers was defined by analogy to heat exchangers as the ratio of the maximum change in the total enthalpy rate of the cold stream to that of the hot stream.

$$\mathrm{HCR} = \left(\frac{\Delta \dot{H}_{\max,c}}{\Delta \dot{H}_{\max,h}} \right) \tag{9.5}$$

The maximum changes are defined by identifying the ideal states that either stream can reach at the outlet of the device. For example, the ideal state that a cold stream can reach at the outlet will be to match the inlet temperature of the hot stream and that a hot stream can reach at the outlet will be to match the inlet temperature of the cold stream. The physics behind this definition is explained in detail in a prior publication [25].

9.2.1 Design Models

HME devices can be studied under the constraint of a fixed performance (with size varying to maintain this performance under varying inlet conditions) or as a fixed piece of hardware (with varying performance under varying inlet conditions). The former is known as an on-design analysis and the latter is known as an off-design analysis. Here we review an on-design model developed in previous work [26, 28] - the energy effectiveness model.

Effectiveness model

An energy-based effectiveness, analogous to the effectiveness defined for heat exchangers, is given as:

$$\varepsilon = \frac{\Delta \dot{H}}{\Delta \dot{H}_{\max}} \tag{9.6}$$

This definition is based on the maximum change in total enthalpy rate that can be achieved in an adiabatic heat and mass exchanger. It is defined as the ratio of change in total enthalpy rate ($\Delta \dot{H}$) to the maximum possible change in total enthalpy rate ($\Delta \dot{H}_{max}$). The maximum possible change in total enthalpy rate can be of either the cold or the hot stream, depending on the heat capacity rate of the two streams. The stream with the minimum heat capacity rate dictates the thermodynamic maximum amount of heat transfer that

can be attained between the fluid streams. This concept is explained in detail in a previous publication [26]. Thus,

$$\Delta\dot{H}_{\max} = \min(\Delta\dot{H}_{\max,c}, \Delta\dot{H}_{\max,h}) \tag{9.7}$$

9.2.2 Analysis of Existing Embodiments of the HDH System

From the literature review, it has been found that no study has carried out a detailed thermodynamic analysis in order to optimize the system performance of existing HDH cycles for either the water and air heated designs. In this chapter, the thermodynamic performance of these HDH cycles is analyzed by way of a theoretical cycle analysis. Control-volume based models for the humidifier and the dehumidifier are used to perform this analysis. The governing equations for the control-volume based models are presented in detail in previous publications [22, 26].

In performing the analysis, the following approximations have been made:

- The processes operate at steady-state conditions.
- There is no heat loss from the humidifier, the dehumidifier, or the heater to the ambient.
- Pumping and blower power is negligible compared to the energy input in the heater.
- Kinetic and potential energy terms are neglected in the energy balance.
- The water condensed in the dehumidifier is assumed to leave at a temperature which is the average of the humid air temperatures at inlet and outlet of the dehumidifier.
- It was previously shown that the use of pure water properties instead of seawater properties does not significantly affect the performance of the HDH cycle at optimized mass flow rate ratios [33]. Hence, only pure water properties are used in the present discussion.

9.2.2.1 Water Heated HDH Cycle

One of the most commonly studied HDH cycles is the closed-air open-water water-heated (CAOW) cycle (see Figure 9.6). A comprehensive study of parameters which affect the performance of this cycle has not been reported in literature. Such a study will help to understand the ways by which the performance of this basic cycle

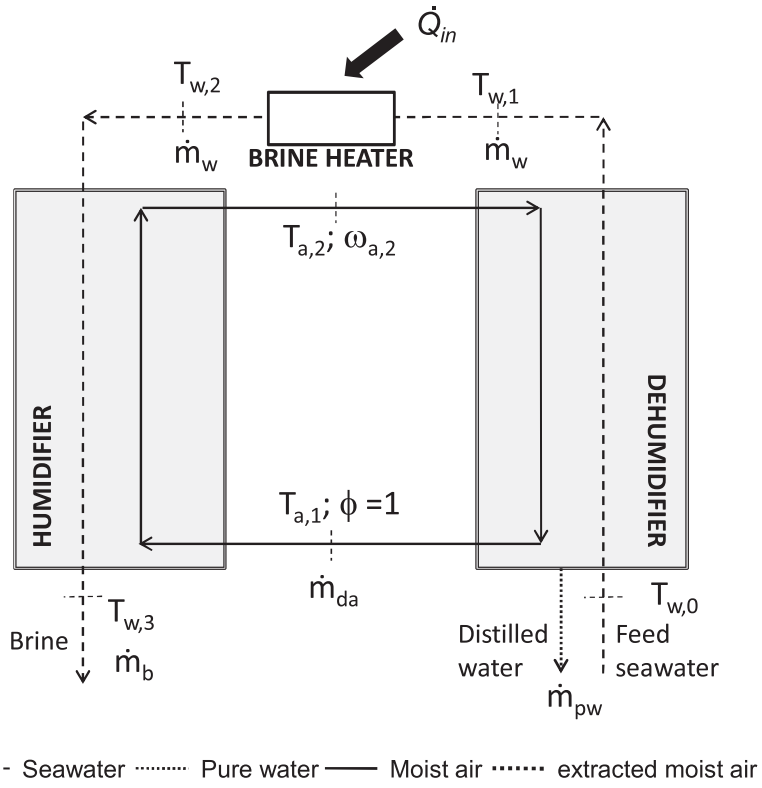

Figure 9.6 Schematic diagram of a water-heated closed-air open-water HDH cycle [22].

can be improved and hence, is reported below. The parameters studied include top and bottom temperatures of the cycle, mass flow rate of the air and water streams, the humidifier and dehumidifier effectivenesses and the operating pressure. The performance of the cycles depends on the mass flow rate ratio (ratio of mass flow rate of seawater at the inlet of the humidifier to the mass flow rate of dry air through the humidifier), rather than on individual mass flow rates. Hence, the mass flow rate ratio is treated as a single variable. This variation with mass flow rate ratio has been noted by many investigators [33, 35–37].

Effect of relative humidity of the air entering and exiting the humidfier ($\varphi_{a,1}$, $\varphi_{a,2}$)

The humidifier and dehumidifier can readily be designed such that the relative humidity of air at their exit is one. Hence, the exit air from these components is usually considered to be saturated

when analyzing these cycles. However, the exit relative humidity is indicative of the performance of the humidifier and the dehumidifier; and hence, understanding how the variation of these parameters changes the performance of the system is important.

Figure 9.7 illustrates the effect that relative humidity of air at the humidifier inlet and exit can have on the performance of the cycle (GOR). For this particular case, the top $(T_{w,2})$ and bottom temperatures $(T_{w,0})$ were fixed at 80°C and 35°C respectively. Humidifier and dehumidifier effectivenesses $(\varepsilon_h, \varepsilon_d)$ were fixed at 90%. Mass flow rate ratio was fixed at 5. It can be observed that for a variation of $\varphi_{a,2}$ from 100 to 70% the performance of the system (GOR) decreases by roughly 3%, and for the same change in $\varphi_{a,2}$ the effect is roughly 34%.

This difference suggests that the relative humidity of the air at the inlet of the humidifier has a much larger effect on performance. These trends were found to be consistent for all values of mass flow rate ratios, temperatures and component effectivenesses. This, in turn, suggests that the dehumidifier performance will have a larger impact on the cycle performance. This issue is further investigated in the following paragraphs.

Effect of component effectiveness (ε_h, ε_d)

Figure 9.8 and 9.9 illustrate the variation of performance of the cycle at various values of component effectivenesses. In Fig. 9.8, the top

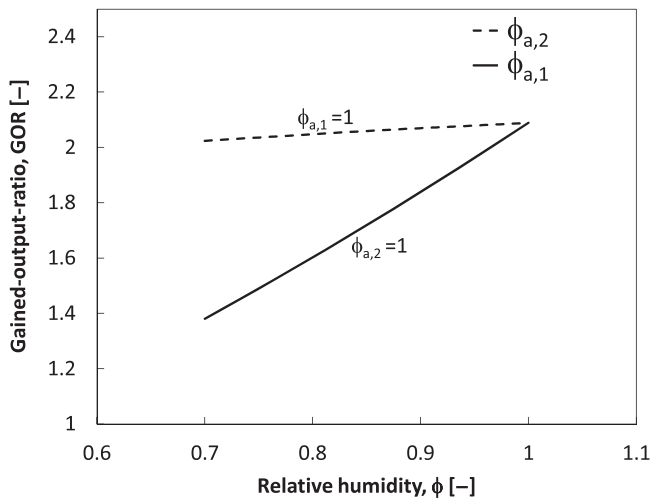

Figure 9.7 Effect of relative humidity on performance of the WH-CAOW HDH cycle [22].

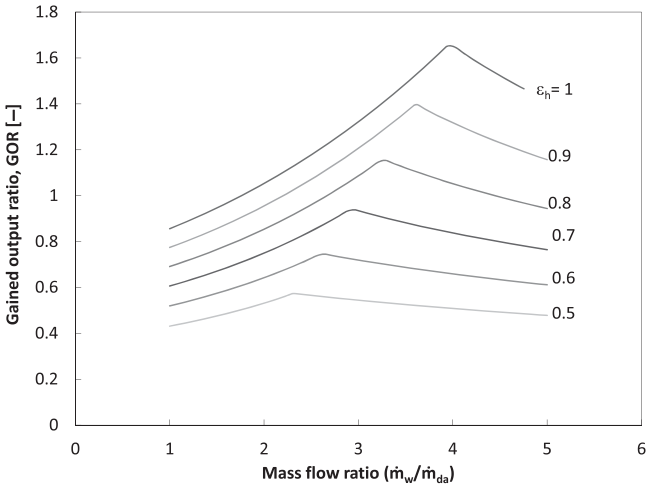

Figure 9.8 Effect of component effectiveness of humidifier on performance of the WH-CAOW HDH cycle [22].

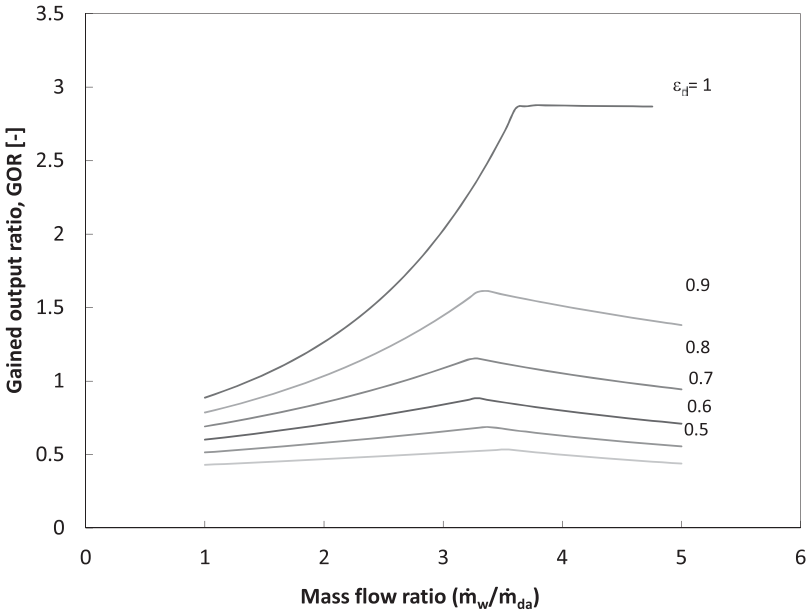

Figure 9.9 Effect of component effectiveness of dehumidifier on performance of the WH-CAOW HDH cycle [22].

temperature is fixed at 80°C, the bottom temperature is fixed at 30°C and the dehumidifier effectiveness is fixed at 80%. The mass flow rate ratio was varied from 1 to 6. It is important to observe that there exists an optimal value of mass flow rate ratio at which the GOR

peaks. It can also be observed that the increase in performance is fairly linear with increasing humidifier effectiveness, ε_h. In Fig. 9.9, the top temperature is fixed at 80°C, the bottom temperature is fixed at 30°C and the humidifier effectiveness is fixed at 80%. The cycle performance changes more dramatically for higher values of dehumidifier effectiveness. These trends are consistent for various values of top and bottom temperatures. Hence, a higher dehumidifier effectiveness is more valuable than a higher humidifier effectiveness for the performance (GOR) of the cycle.

In the previous discussion, we have observed that the dehumidifier exit air relative humidity ($\varphi_{a,1}$) is more important than the humidifier exit air relative humidity ($\varphi_{a,2}$). Hence, based on these results, we can say that for a water heated cycle the performance of the dehumidifier is more important than the performance of the humidifier.

Effect of top temperature ($T_{w,2}$)

Figure 9.10 illustrates the effect of the top temperature on the cycle performance (GOR). For this particular case, the bottom temperature ($T_{w,0}$) was fixed at 35°C and humidifier and dehumidifier

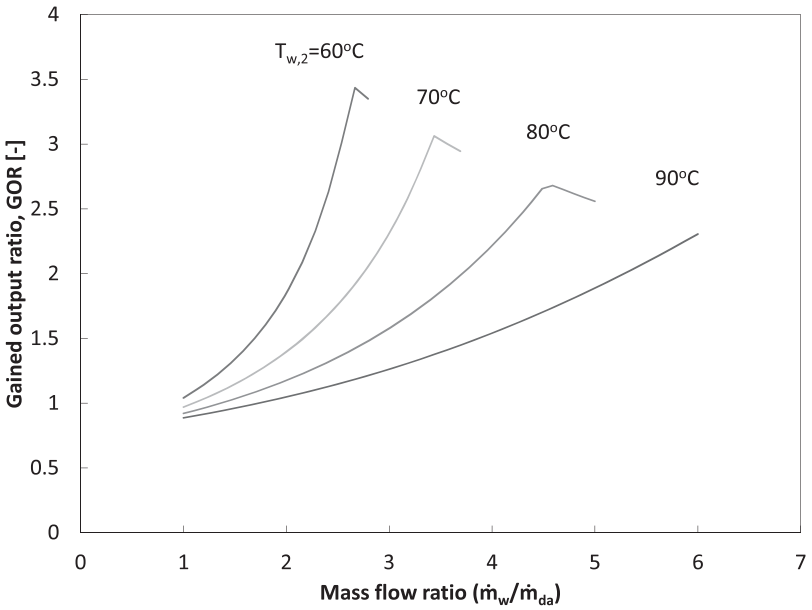

Figure 9.10 Effect of top brine temperature on performance of the WH-CAOW HDH cycle [22].

effectivenesses were fixed at 92%. Top temperature ($T_{w,2}$) was varied from 50°C to 90°C. The optimal value of mass flow rate ratio increases with an increase in top temperature. Depending on the humidifier and dehumidifier effectiveness itself this trend changes. At lower component effectivenesses, the top temperature has no or little effect on the cycle performance. This result is counter-intuitive. However, it can be explained using the modified heat capacity rate ratio.

The modified heat capacity rate ratio (HCR) as the ratio of maximum possible enthalpy change in the cold stream to the maximum possible enthalpy change in the hot stream. It was found that the entropy generation in a heat and mass exchange device is minimized (for a given effectiveness and inlet conditions) when HCR=1 (' balanced' condition). We are going to use this understanding here to explain the trends obtained at various top temperatures.

Figure 9.11 shows the variation of GOR with the heat capacity rate ratio of the dehumidifier ($\mathrm{HCR_d}$). It can be seen that GOR reaches a maximum at $\mathrm{HCR_d} = 1$. The maximum occurs at a balanced condition for the dehumidifier which, as we have shown in the preceeding paragraphs is the more important component. Further, it

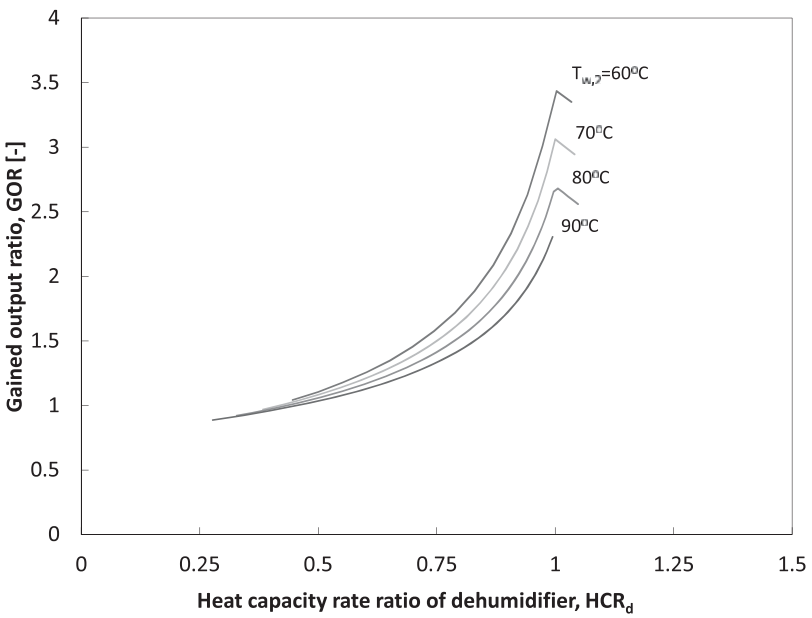

Figure 9.11 HCR of dehumidifer versus GOR at various top brine temperatures [22].

can be noticed from Fig. 9.12 that the degree of balancing of the humidifier at the optimum GOR condition reduces (HCR_h moves farther away from 1) as the top temperature increases. Hence, the irreversibility of the humidifier (and the total irreversibility of the system) increases with increase in top temperature. A system with higher total irreversibility has a lower GOR [33]. This explains the decrease in GOR with an increase in top temperature.

Also, as the top temperature increases, the dehumidifier is balanced at higher mass flow ratio and hence the optimum value of GOR occurs at higher mass flow ratios.

Effect of bottom temperature ($T_{w,0}$)

The bottom temperature of the cycle ($T_{w,0}$) is fixed by the feedwater temperature at the location where the water is drawn. Figure 9.13 illustrates a case with top temperature of 80°C and component effectivenesses of 92%. A higher bottom temperature of the cycle results in a higher value of GOR as illustrated in the figure. This result can again be understood by plotting HCR of humidifier and dehumidifier versus the GOR of the system (Figs. 9.14 and 9.15).

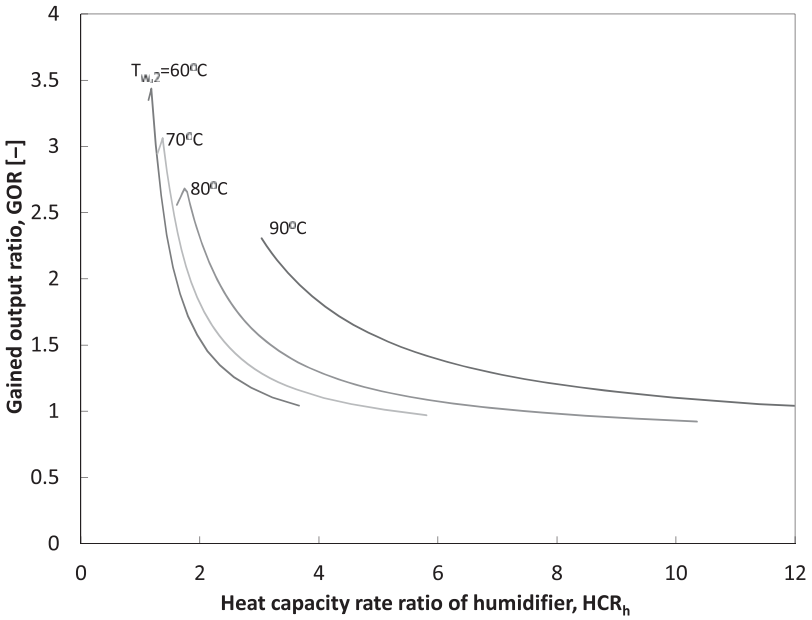

Figure 9.12 HCR of humidifier versus GOR at various top brine temperatures [22].

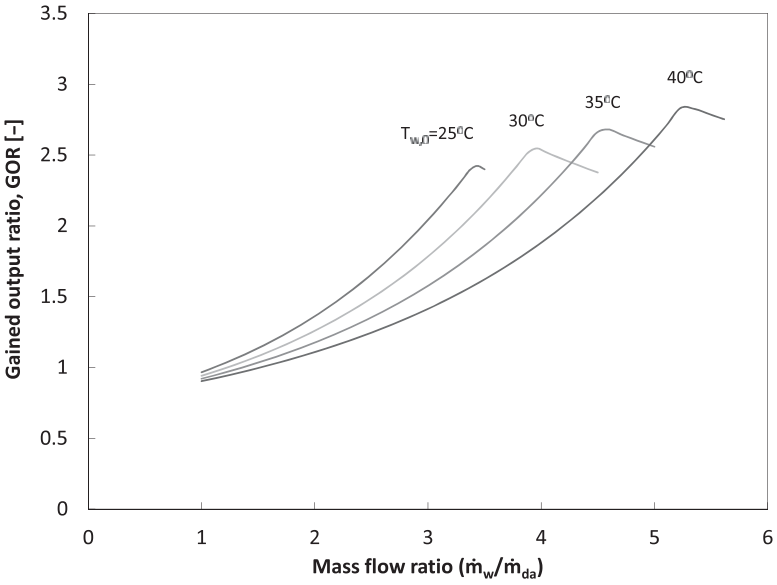

Figure 9.13 Effect of feedwater temperature on performance of the WH-CAOW HDH cycle [22].

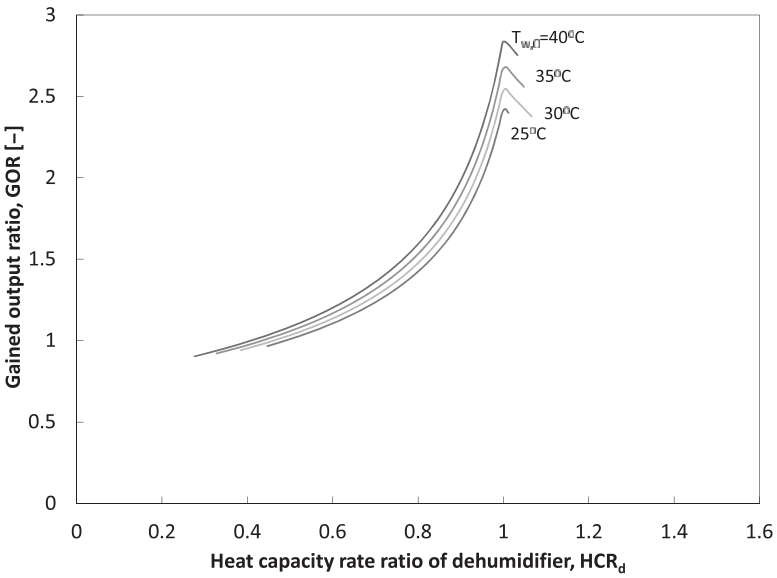

Figure 9.14 HCR of dehumidifer versus GOR at various feedwater temperatures [22].

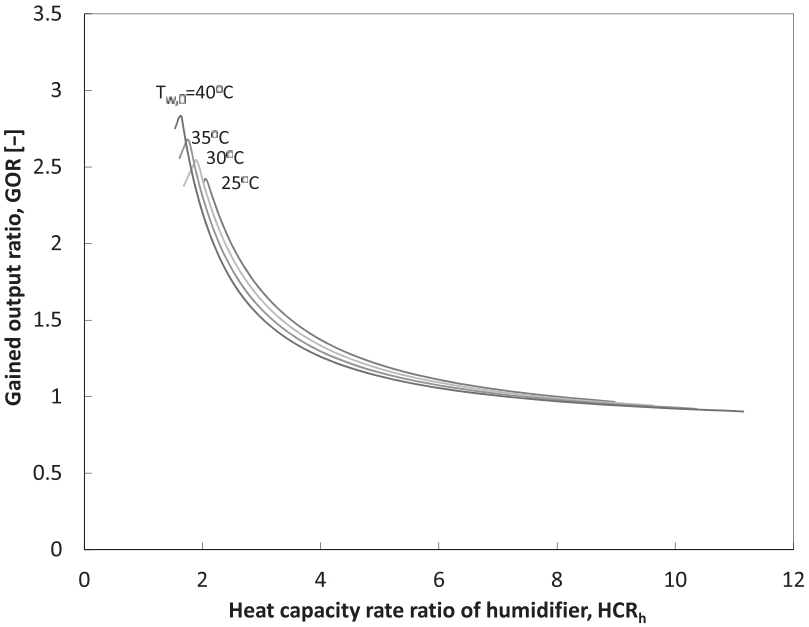

Figure 9.15 HCR of humidifier versus GOR at various feedwater temperatures.

The degree of balancing of the humidifier at the optimum condition for GOR decreases with a decrease in bottom temperature. Hence, the irreversibilities in the humidifier (and the total irreversibility of the system) increase with decreasing bottom temperature, and the GOR declines.

From the discussions in this subsection we have observed that the performance of the cycle (GOR) has a functional dependence as follows:

$$\text{GOR} = f(\text{HCR}_h, \text{HCR}_d, \varepsilon_h, \varepsilon_d, T_{w,2}, T_{w,0}, \varphi_{a,2}, \varphi_{a,1}) \qquad (9.8)$$

The numerically computed values of GOR reported in this section for the CAOW water-heated cycle are within 20% of the experimental value obtained by Nawayseh [38] for the same boundary conditions. Further experimental validation is presented later in this section.

9.2.2.2 Single and Multi-Stage Air Heated Cycle

A simple [23, 24, 39, 40] air-heated cycle is one in which air is heated, humidified, and dehumidified. Current simulations have found that the GOR for this cycle is very low (GOR<1; only slightly better than a solar still). It is important to understand the reasons for this poor performance. The air in this cycle is heated and immediately

sent to a humidifier where it is saturated. The air also gets cooled during the humidification process since it is at a higher temperature than the water stream. Thus, heat is lost to the water stream in the humidifier. In the water-heated cycle, the air stream is heated in the humidifier. This further facilitates heat recovery in the dehumidifier, which is absent in an air heated system. Hence, the performance is much lower in an air-heated system.

To improve the performance of air-heated systems, Chafik [23, 41] proposed a multi-stage cycle. The air in this cycle is heated and sent to a humidifier where it is saturated. It is then further heated and humidified again. The idea behind this scheme was to increase the exit humidity of the air so that water production can be increased. Chafik was able to increase the exit humidity from 4.5% (by weight) for a single stage system to 9.3% for a 4 stage system. We reproduce this result for the same cycle under similar operating conditions. However, we also observe that the GOR of the cycle rises by only 9% (Fig. 9.16). This is because the increased water production comes at the cost of increased energy input. This, in turn, is because the multi-staging does not improve the heat recovery in the humidification process. Chafik reported

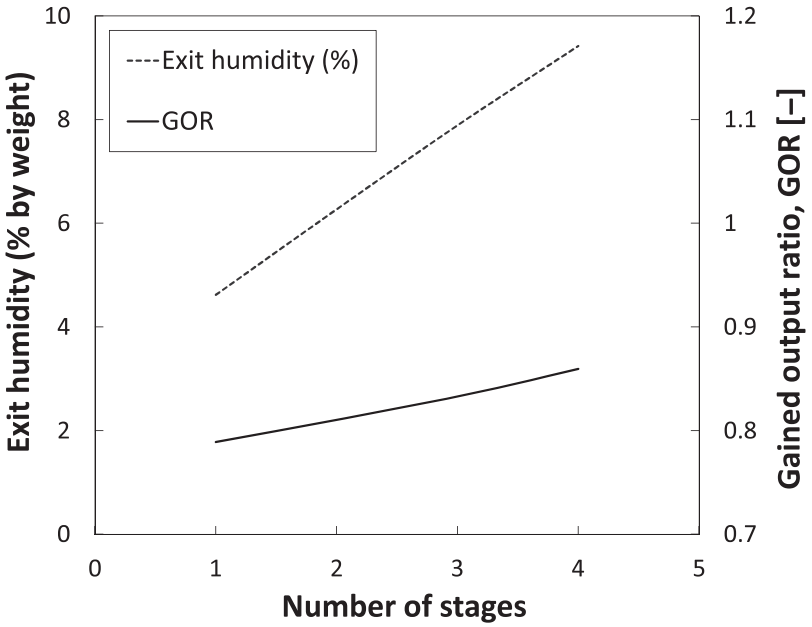

Figure 9.16 Effect of number of stages on performance of air heated CAOW HDH system [22].

very high cost of water production of 28.65 Euro/m^3 caused in part by the low energy efficiency of the system.

9.2.2.3 Summary

In this section, we have examined the effect of a number of parameters and configurations on the performance of basic HDH cycles. The following significant conclusions are reached:

1. The performance of a basic water-heated cycle depends on: (a) the water-to-air mass flow rate ratio; (b) the humidifier and dehumidifier effectivenesses; (c) top and bottom temperatures; and (d) relative humidity of air at the exit of the humidifier and the dehumidifier.
2. At a specific value of the water-to-air mass flow rate ratio, the performance of the system is optimal. This optimal point is characterized by a thermodynamically balanced condition in the dehumidifier. The balanced condition, as explained previously, occurs at a modified heat capacity rate ratio of 1. This finding is important, as it is also fundamental to design algorithms for HDH systems with mass extraction and injections.
3. As shown in the table below, previously studied multi-stage and single-stage air heated cycles have low energy efficiency compared to the water heated HDH cycle.
4. The performance of existing HDH systems is only about $1/60^{th}$ of the thermodynamically reversible GOR. This shows the extent of the thermodynamic losses in these systems. Much of the remainder of this chapter is dedicated to improving the thermal design of the HDH cycle so as to reduce the thermodynamic irreversiblity.

Table 9.1 Comparison of GOR of HDH cycles under representative boundary conditions.

CYCLE	GOR
Single stage air heated cycle	0.78
Four-stage air heated cycle	0.85
Water heated cycle	2.5
Reversible cycle	122.5

9.2.3 Systems with Mass Extraction and Injection

Studies have been conducted on the effect of entropy generation on the thermal design of the HDH system [29, 33, 42, 43], and it has been found that reducing the total entropy generated (per unit amount of water distilled) improves the energy efficiency (measured in terms of the gained-output-ratio or GOR). It has also been reported that incorporating mass extractions and injections to vary the water-to-air mass flow rate ratio in the combined heat and mass transfer devices (like the humidifier and the dehumidifier) can potentially help in reducing entropy production in those devices [25]. A comprehensive method of thermodynamic analysis is available for the design of mass extractions and injections in the HDH system. This approach (discussed in the subsequent sections) draws upon the fundamental observation that there is a single value of water-to-air mass flow rate ratio (for any given boundary conditions and component effectivenesses) at which the system performs optimally [22].

A schematic diagram of a representative the HDH system with mass extractions and injections is shown in Fig. 9.17. The system shown here is a water-heated, closed-air, open-water system with three air extractions from the humidifier into the dehumidifier. States a to d are used to represent various states of the seawater stream and states e and f represent that of moist air before and after dehumidification. Several other embodiments of the system are possible based on the various classifications of HDH listed earlier in this chapter.

Enthalpy pinch model

McGovern et al. [44] proposed that it is advantageous to normalize enthalpy rates by the amount of dry air flowing through the system for easy representation of the thermodynamic processes in enthalpy versus temperature diagrams. We use this concept here and derive the following equation from Eq. (9.6) by dividing the numerator and the denominator by the mass flow rate of dry air ($\dot{m}_{da}$):

$$\varepsilon = \frac{\Delta h^*}{\Delta h^*_{\max}} \tag{9.9}$$

$$= \frac{\Delta h^*}{\Delta h^* + \Psi_{TD}} \tag{9.10}$$

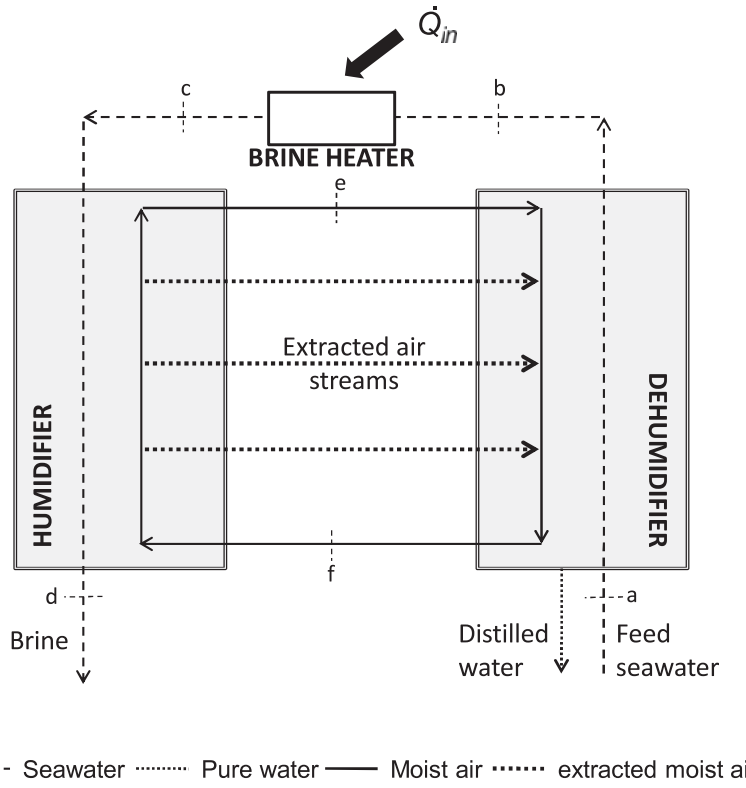

Figure 9.17 Schematic diagram of a water-heated, closed-air, open-water humidification-dehumidification desalination system with mass extraction and injection of the moist air stream [28].

Ψ_{TD} is the loss in enthalpy rates at terminal locations because of having a "finite-sized" HME device, and it is defined as follows:

$$\Psi_{TD} = \min\left(\frac{\Delta\dot{H}_{\max,c}}{\dot{m}_{da}} - \Delta h^*, \frac{\Delta\dot{H}_{\max,h}}{\dot{m}_{da}} - \Delta h^*\right) \quad (9.11)$$

$$= \min(\Psi_c, \Psi_h) \quad (9.12)$$

In the case of a heat exchanger, Ψ_{TD} will be analogous to the minimum terminal stream-to-stream temperature difference (TTD). TTD is seldom used to define performance of a heat exchanger in thermodynamic analyses; the temperature pinch is the commonly used parameter. The difference is that pinch is the minimum stream-to-stream

temperature difference at any point in the heat exchanger and not just at the terminal locations. Like temperature pinch, Ψ can be defined as the minimum loss in enthalpy rate due to a finite device size at any point in the HME device and not just at the terminal locations. Thus, the general definition of Ψ will be as follows:

$$\Psi = \min_{local}(\Delta h^{*}_{\max} - \Delta h^{*}) \tag{9.13}$$

Hence, based on the arguments presented in this section, we can say that Ψ for an HME device is analogous to temperature pinch for a heat exchanger, and it can be called the 'enthalpy pinch'. We recommend that, because of the presence of the concentration difference as the driving force for mass transfer in HME devices, a temperature pinch or a terminal temperature difference should not be used when defining the performance of the device. Further details about the enthalpy pinch and its significance in thermal design of HME devices are given in detail in Reference [28]. Balancing of HDH cycles has been studied in further detail in References [30], [31], and [45].

9.2.3.1 System Balancing Algorithms

In a previous publication, we used the concepts of thermodynamic balancing developed for HME devices and applied them to the HDH system design [28]. Detailed algorithms for systems with zero, single, and infinite extractions were developed. Temperature-enthalpy diagrams were used to model the systems. Figure 9.18 illustrates temperature versus enthalpy of a system with a single extraction and injection. In the illustrated case, the air was extracted from the humidifier at the state 'ex' and injected in a corresponding location in the dehumidifier with the same state 'ex' to avoid generating entropy during the process of injection. This criteria for extraction is applied for all the cases reported in this paper since it helps us study the effect of thermodynamic balancing, independently, by separating out the effects of a temperature and/or a concentration mismatch between the injected stream and the fluid stream passing through the HME device (which when present can make it hard to quantify the reduction in entropy generated due to balancing alone).

The effect of the number of extractions (at various enthalpy pinches) on the performance of the HDH system was studied using the developed algorithms and is shown in Fig. 9.19. Several important observations can be made from this chart.

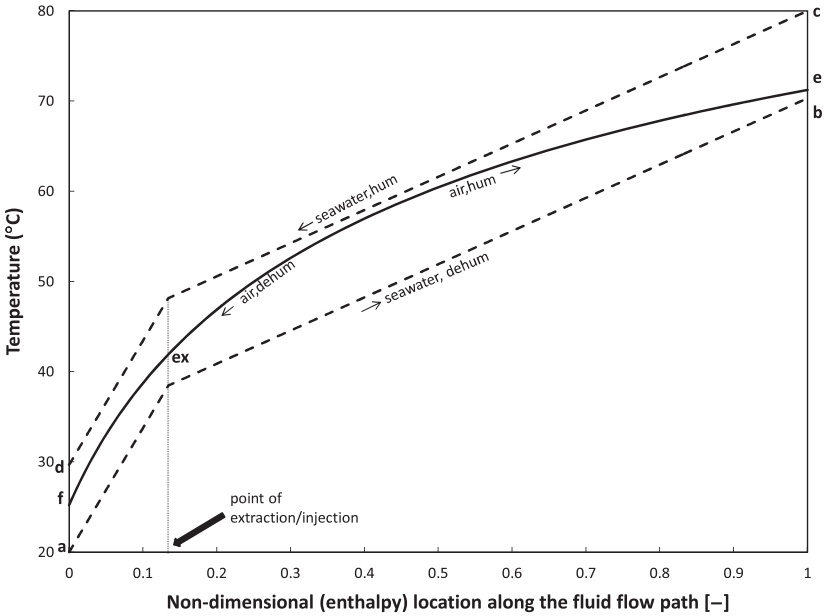

Figure 9.18 Temperature profile representing the HDH system with a single extraction. Boundary conditions: $T_a = 20^\circ$ C; $T_c = 80^\circ$ C; $\Psi_{deh} = \Psi_{hum} = 20$ kJ/kg dry air [28].

First, it may be observed that thermodynamic balancing is effective in HDH cycles only when the humidifier and the dehumidifier have an enthalpy pinch less than about 27 kJ/kg dry air. For various boundary conditions, it has been found that above the aforementioned value of enthalpy pinch the difference in performance (GOR) with that of a system without any extractions or injections is small (less than 20%). Further, at very low values of the enthalpy pinch ($\Psi \leq 7$ kJ/kg dry air) in the humidifier and the dehumidifier, the limiting case of continuous balancing with infinite number of extractions and injections was found to give much better results than that with a single extraction and injection. For a top brine temperature of 80°C, a feed water temperature of 20° C and 'infinitely' large humidifier and dehumidifier ($\Psi_{hum} = \Psi_{deh} = 0$ kJ/kg dry air), the GOR was found to be 8.2 for a single extraction (compared to a GOR of 109.7 for a similar system with an infinite number of extractions, i.e. continuous extraction). At higher values of enthalpy pinch ($7 < \Psi \leq 15$), a single extraction reduced the entropy generation of the total system roughly by a similar amount as continuous extractions. At even higher values of enthalpy pinch ($15 < \Psi \leq 27$), a single extraction outperforms continuous extractions.

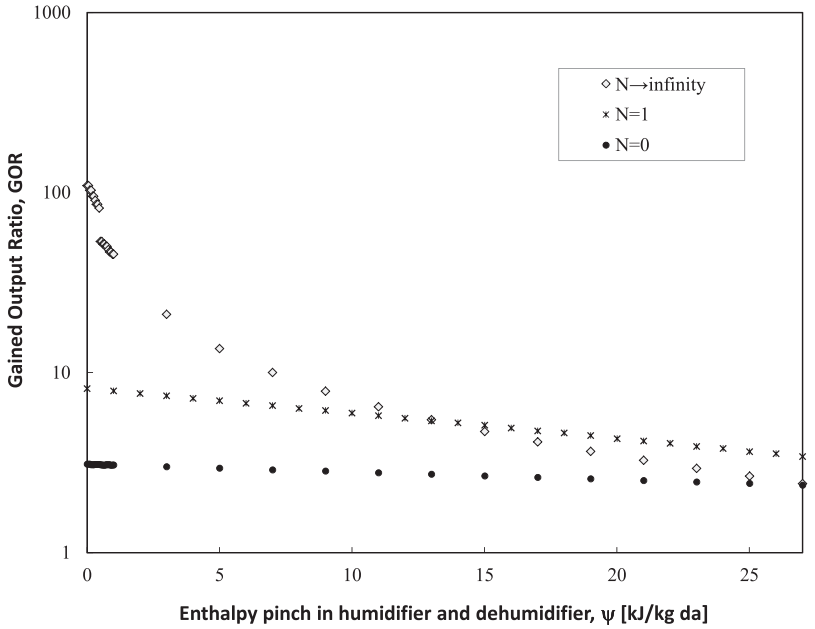

Figure 9.19 Effect of number of extractions (for thermodynamic balancing) on the performance of the HDH system with finite and infinite size HME devices. Boundary conditions: $T_a = 20^\circ$C; $sal = 35$ g/kg; $T_c = 80^\circ$C; HCR_{deh}=1 [28].

9.2.4 Experimental Realization of HDH with Extraction

A pilot scale HDH unit producing up to 700 liters of pure water per day has been built [29]. The unit was fully instrumented and both component and system experiments were carried out.

9.2.4.1 HME Balancing

As described previously, theoretical considerations show that a modified heat capacity rate ratio (HCR) of 1 will lead to minimum entropy generation in a fixed effectiveness or fixed hardware device [25, 26, 29] and that the condition should be established to optimize the thermal performance of the HDH cycle [22]. In this section, this important conclusion is investigated experimentally.

Figure 9.20 illustrates that there exists a particular mass flow rate at which non-dimensional entropy generated in the device is minimized (fixed inlet air condition and fixed inlet water temperature). At different values of these boundary conditions, the same result was found to be true. The minimum that is observed also

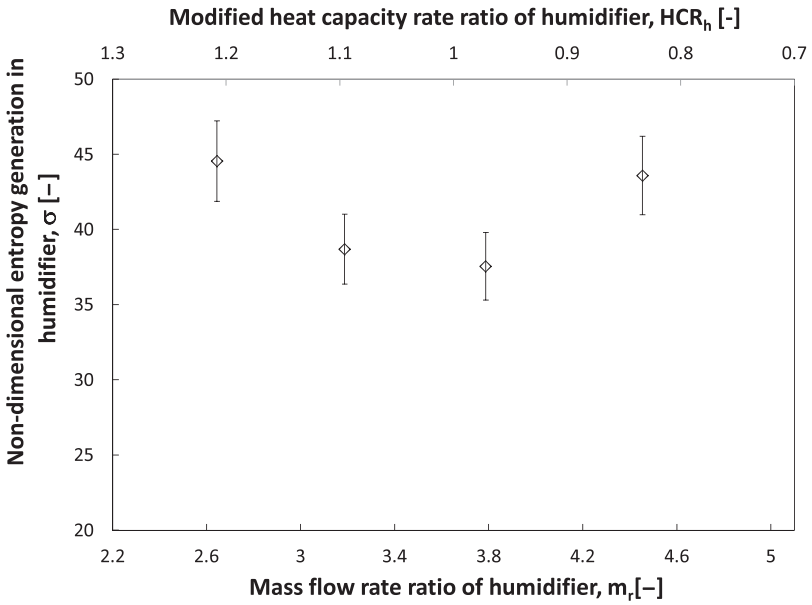

Figure 9.20 Effect of mass flow rate ratio on non-dimensional entropy generation in the humidifier. Boundary conditions: $T_e = 32^\circ$C; T_c =60°C; $T_{wb,e} = 20^\circ$C; $P = 101.3$ kPa; $V_h = 0.27$ m^3[29].

corresponds to the case closest to an HCR of 1. This is consistent with the theoretical observation that irreversiblity is minimized at HCR of unity [25, 27, 29].

9.2.4.2 System Balancing

Figure 9.21 illustrates the effect of mass flow rate extracted on the increase in performance of the HDH system. The increase in performance of the HDH system is calculated as the ratio of the GOR with extraction to that without extraction. In cases with and without extraction the top brine temperature, the feedwater temperature, the water flow rate and total air flow entering the humidifier from the dehumidifier (measured at state 'f' shown in Fig. 9.3) are held fixed. In the zero extraction case, this aforementioned ratio of GORs is 1 and increases with better balancing. The amount of air extracted is also normalized against total air flow.

It may be observed that the performance is optimal at a particular amount of extraction. In this particular case, where the top temperature is 90°C and the feed temperature is 25°C, the optimum amount of extraction is around 33%. The GOR is enhanced by up

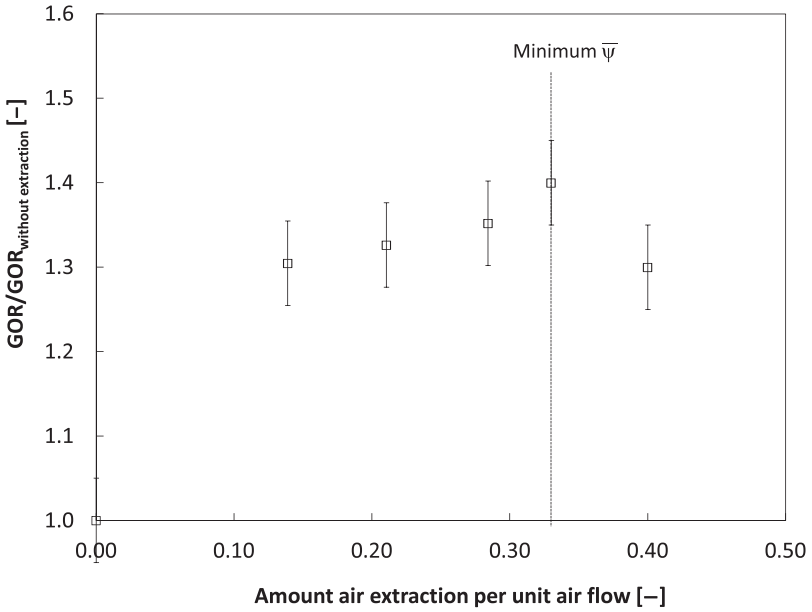

Figure 9.21 Effect of mass flow rate of air extracted on the performance of the HDH system. Boundary conditions: $T_a = 25^\circ$ C; $T_c = 90^\circ$ C; $N = 1$; $V_h = 0.27$ m^3; $A_d = 8$ m^2[29].

to 40%. The trends are similar at different boundary conditions and the maximum enhancement in GOR with a single extraction of air was found to be about 55%.

As would be expected, the maximum performance corresponded to the minimum average of local enthalpy pinches in the dehumidifier ($\overline{\Psi}_{local,d}$). This is consistent with the principal purpose of thermodynamic balancing: to drive the process at minimum driving force and correspondingly smaller entropy generation at a fixed system size.

9.2.4.3 Summary of HDH Characteristics Related to Extraction

1. HCR=1 (i.e. the point at when the maximum change in enthalpy rates of either stream exchanging energy is equal) represents a thermally balanced state for a simultaneous heat and mass exchange device.
2. For a water heated CAOW HDH system without mass extractions, the HCR$_d$=1 represents the state at which the GOR is maximized.

3. HDH systems without mass extractions need to be operated at as high a top brine temperature as is possible in order to ensure a high GOR.
4. Mass extractions from the humidifier to the dehumidifier increase the GOR of the water heated CAOW HDH system by up to 55%.
5. It is found that thermodynamic balancing is effective in HDH only when the HME devices have an appropriately low enthalpy pinch ($\Psi < 27$ kJ/kg dry air).
6. The optimum extraction mass flow rate corresponds to the case in which a minimum average local enthalpy pinch is achieved in the device.

9.3 Bubble Column Dehumidification

When a non-condensable gas is present, the thermal resistance to condensation of vapor on a cold surface is much higher than in a pure vapor environment. This is, primarily, caused by the diffusion resistance to transport of vapor through the mixture of non-condensable gas and vapor. Several researchers have previously studied and reported this effect [46–54]. When even a few mole percent of non-condensable gas are present in the condensing fluid, the deterioration in the heat transfer rates can be up to an order of magnitude [56–60]. From experimental reports in literature, it can be observed that the amount of deterioration in heat transfer is a very strong (almost quadratic) function of the mole fraction of non-condensable gas present in the condensing vapor.

In HDH systems, a large percentage of air (60–90% by mass) is present by default in the condensing stream. As a consequence, the heat exchanger used for condensation of water out of an air-vapor mixture (otherwise known as adehumidifier) has very low heat and mass transfer rates (an 'equivalent' heat transfer coefficient as low as 1 W/m^{2}K in some cases [19, 61–63]). This leads to very high heat transfer area requirments in the dehumidifier (up to 30 m^2 for a 1 m^2/day system). In this section, we describe how to achieve a substantial improvement in the heat transfer rate by condensing the vapor-gas mixture in a column of cold liquid, rather than on a cold surface, by using a bubble column heat and mass exchanger.

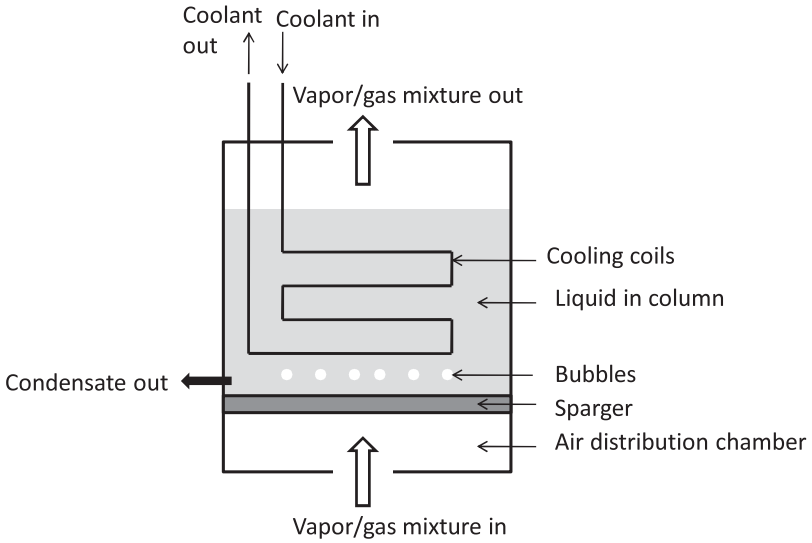

Figure 9.22 Schematic diagram of the bubble column dehumidifier [66].

In this device, moist air is sparged through a porous plate (or any other type of sparger [64]) to form bubbles in a pool of cold liquid. The upward motion of the air bubbles causes a wake to be formed underneath the bubble which entrains liquid from the pool, setting up a strong circulation current in the liquid pool [65]. Heat and mass are transferred from the air bubble to the liquid in the pool in a direct contact transport process. At steady state, the liquid, in turn, losses the energy it has gained to the coolant circulating through a coil placed in the pool for the purpose of holding the liquid pool at a steady temperature. The system is illustrated in Fig. 9.22.

9.3.1 Modeling and Experimental Validation

A thermal resistance models for the condensation of water from an air-vapor mixture in a bubble column heat exchanger were introduced in Reference [66] and have been revised and refined in References [67-69]. The primary temperatures in the resistance network are: (1) the average local temperature of the air-vapor mixture in the bubbles (T_{air}), (2) the average temperature of the liquid in the pool (T_{column}), [64] and (3) the average local temperature of the coolant inside the coil ($T_{coolant}$). Between T_{air} and T_{column} there

is direct contact heat and mass transfer. The liquid pool is well-mixed by the bubbles, and may be considered to hold a constant temperature. The local heat transfer from the pool to the coolant can be represented by heat transfer coefficients inside and outside the coil, and the temperature change of the coolant can be modeled as a single-stream heat exchanger. The heat transfer between the moist air stream may be modeled similarly.

Figure 9.23 illustrates an example of the experimental and modeling results [66]. A strong effect of the mole fraction is seen, as is also the case in steam condensers. From the experiments, we observe that the effect is more linear than quadratic (in the studied range). Hence, the presence of non-condensable gas is affecting the heat transfer to a much lesser degree than in the film condensation situations of a standard dehumidifier. This demonstrates the superiority of the bubble column dehumidifier technology [70]. This observation is further discussed in Sec. 9.3.2. Figure 9.23 also illustrates that the model predicts the effect of inlet mole fraction very accurately.

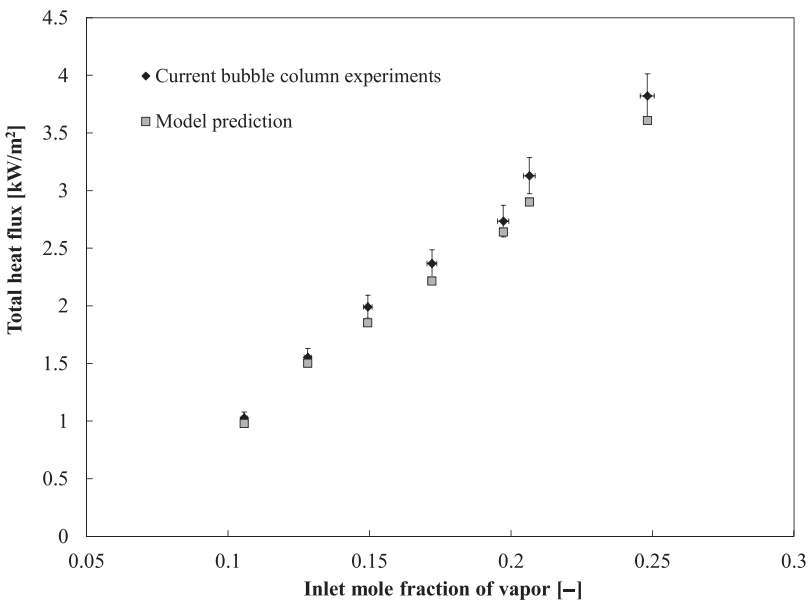

Figure 9.23 Effect of inlet mole fraction of the vapor on the total heat flux in the bubble column measured and evaluated at $Vg = 3.8$ cm/s; $D_b = 4$ mm; $H = 254$ mm [66].

9.3.2 Prototype

In an HDH system, the isothermal nature of the column liquid in the bubble column dehumidifier reduces the temperature to which seawater can be preheated to (in the coils). This limits the energy effectiveness of the device [26]. A low effectiveness in the dehumidifier, reduces the HDH system performance significantly [22]. In this section, we detail an innovation which increases the energy effectiveness of these devices.

A schematic diagram of a multi-stage bubble column is shown in Fig. 9.24. In this device, the moist air is sparged successively from the bottom-most (first) stage to the top-most (last) stage through pools of liquid in each stage. The coolant enters the coil in the last stage and passes through the coil in each stage and leaves from the first stage. Thus, the moist air and the coolant are counter-flowing from stage to stage the condensate is collected directly from the column liquid in each stage.

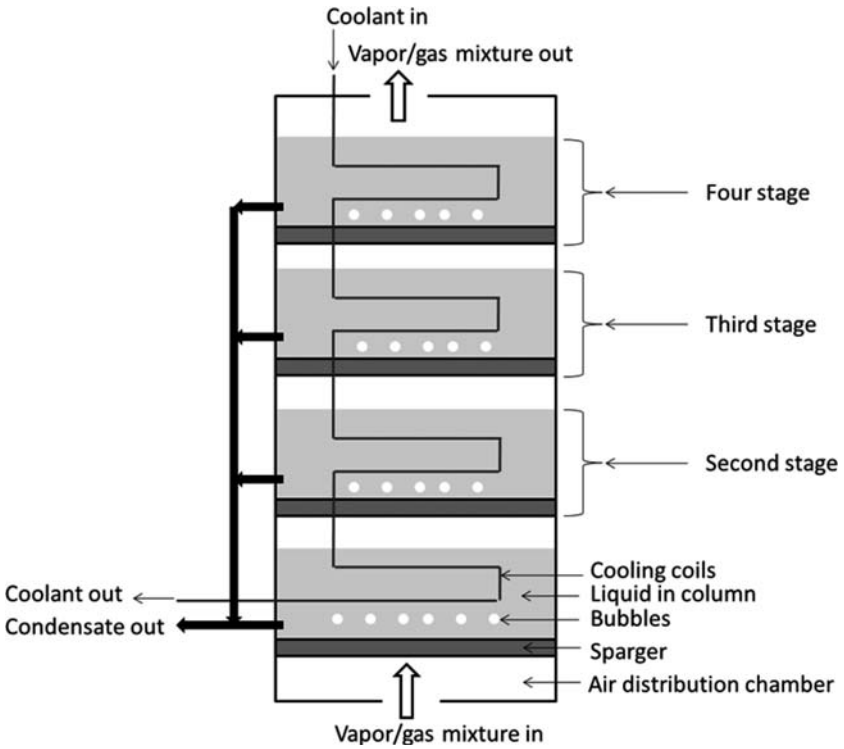

Figure 9.24 Schematic diagram of multi-stage bubble column dehumidifier [66].

Figure 9.25 illustrates the temperature profiles in a single stage and multi-stage bubble column. In both cases, the moist air comes in fully saturated at a temperature of 353 K and leaves dehumidified at 310 K. In the process, the pool of liquid in the bubble column gets

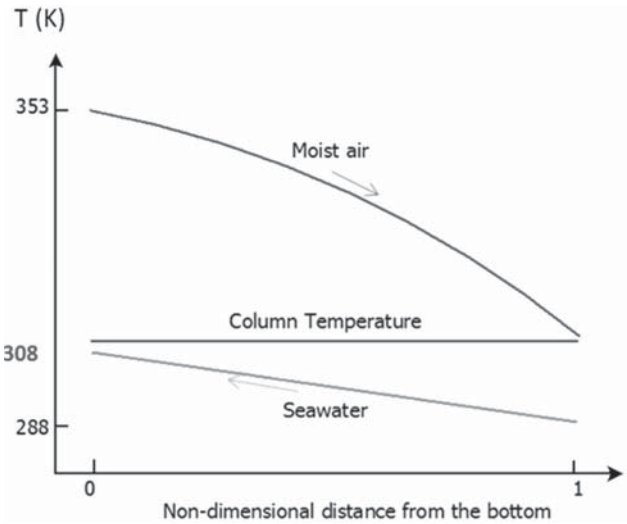

(**a**) Single stage

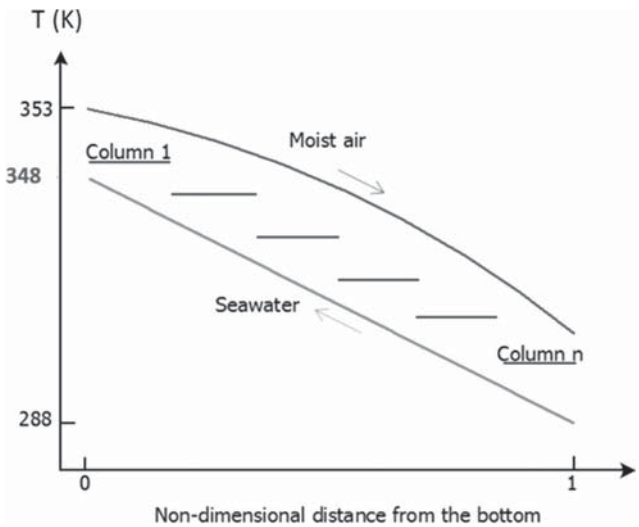

(**b**) Multi-stage

Figure 9.25 An illustration of the temperature profile in the bubble columns for (a) single stage and (b) multi-stage [66].

heated and in turn preheats the seawater going through the coil. In the single stage case, the coolant gets preheated to a temperature of 308 K only (limited by the air exit temperature of 310 K). This corresponds to a very low effectiveness of 30%. In the case of multistage bubble columns, the column liquid in each stage is at a different temperature limited by the temperature of the air passing through the respective stage. Hence, the outlet coolant temperature is only limited by the exit temperature of the air from the first stage. In this example, we see that the coolant reaches 348 K (40 K higher than in the single stage case). This corresponds to an increase in effectiveness from 30% in the single stage device to 92% in the multi-stage device.

Figure 9.26 illustrates the increase in effectiveness of the device with multistaging. The data presented here is for an air inlet temperature of 65°C, inlet relative humidity of 100%, a water inlet temperature of 25°C and a water-to-air mass flow rate ratio of 2.45. It can be seen that the energy effectiveness of the device is increased from around 54% for a single stage to about 90% for the three stage

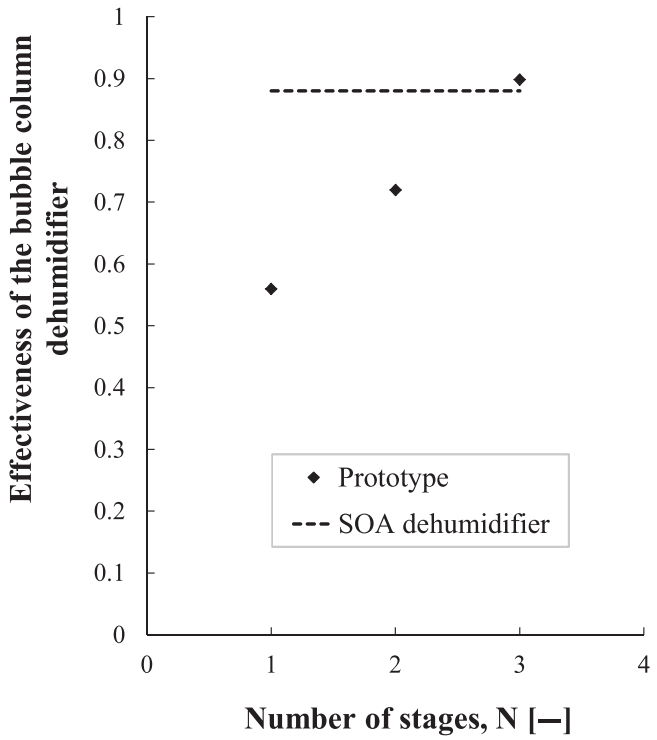

Figure 9.26 Effect of multistaging the bubble column on energy effectiveness of the device.

device. Further, owing to the higher superficial velocity (because of smaller column diameter), the heat fluxes were much higher (up to 25 kW/m^2) than for film-condensation dehumidifiers. Also, the total gas side pressure drop of this device was modest at 800 Pa.

9.3.3 Comparison to Existing Devices

A state-of-the-art dehumidifier (which operates in the film condensation regime) procured from Fischer LLC was found to yield a maximum heat flux of 1.8 kW/m^2 (as per the design specification) compared to a maximum of 25 kW/m^2 obtained in the bubble column dehumidifier, demonstrating the superior performance of the novel device. This comparison was carried out at the same inlet conditions for the vapor-air mixture and the coolant streams. Also, the streamwise temperature differences were similar in both cases. Further, the energy effectiveness of a three-stage bubble column dehumidifier was found to be similar to the conventional dehumidifier mentioned here.

By way of this innovation, the heat transfer area requirement is reduced to a fraction of that in existing HDH systems and is brought close to that for pure vapor systems (such as MED systems). This trend is illustrated in Fig. 9.27.

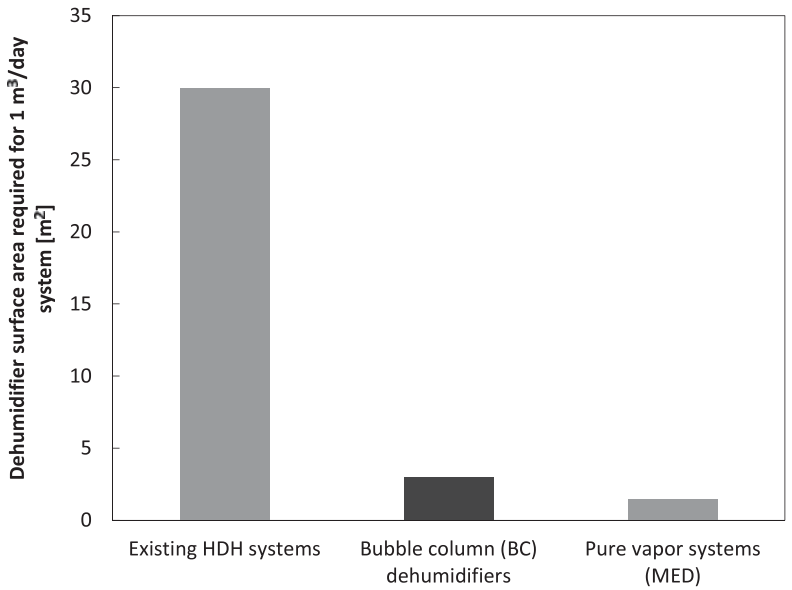

Figure 9.27 Dehumidifier area requirement for bubble columns compared to existing technology.

9.3.4 Summary of Bubble Column Dehumidification in HDH Systems

1. Bubble column dehumidifiers have an order of magnitude better performance than existing state-of-the-art dehumidifiers operating in the film condensation regime.
2. In order to minimize pressure drop, the liquid height can be kept to a minimum such that the coil is entirely submerged in the liquid. This is possible because the height been shown to have no effect on the performance of the device for column heights down to 4 cm [68], and is likely to have minimal effect so long as the pool depth is somewhat greater than the bubble diameter ($\approx$ 4–6 mm).
3. A three-stage bubble column with a manageable air side pressure drop of < 1 kPa, an high effectiveness of 92%, and a very high heat rate of 25 kW/m^2 can be constructed at a fraction of the cost of a regular dehumidifier operating in the film condensation regime.

Implementation of the novel dehumidifier described for application in HDH systems will reduce the capital cost of the system leading to a reduced cost of water production. The volume is reduced to $1/18^{th}$ of the regular dehumidifier.

9.4 Cost of Water Production

The cost of water production is calculated by a standard method used in the desalination industry [71, 72].

Figure 9.28 illustrates a three-dimensional model of a trailer-mounted, single air extraction HDH system operating under sub-atmospheric pressure with a 12 foot (3.6 m) tall packed bed humidifier and a four-stage bubble column dehumidifier. This unit is designed to produce 10 m^3 per day. We have calculated the cost of this unit as an example of the cost of the state-of-the-art in HDH systems.

The total thermal energy consumed by this system is 156 kWh_{th} per cubic meter of water produced and the electrical energy consumption is 1.2 kWh per cubic meter of water produced. The thermal energy is provided from compressed natural gas tanks on the trailer at an assumed cost of $4 per 1000 cubic feet (this is the current average price in India [73]). The electrical energy is provided using a diesel generator at the rate of $0.20 per kWh. The total energy cost per m^3 of water produced is $2.17.

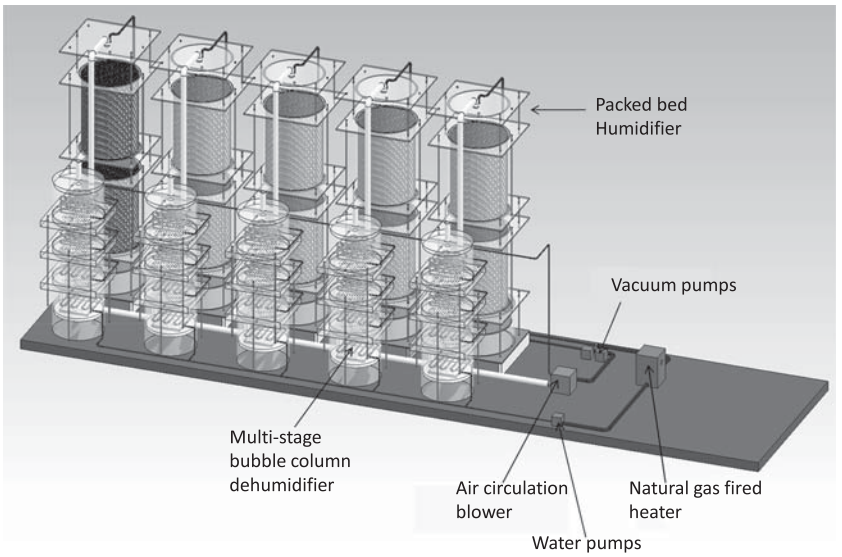

Figure 9.28 Three-dimensional model of a trailer-mounted, sub-atmospheric-pressure, natural-gas-fired, single air extraction HDH system with a 12 foot tall packed bed humidifier and a four-stage bubble column dehumidifier [73].

The capital cost is the sum of the various costs listed in Table 9.2. These costs are obtained from different manufacturers. The parts for the humidifier and dehumidifier are to be obtained from these manufacturers and the assembly and fabrication is to be done by sub-contractors.

The total capital cost is amortized over a life of 20 years. The amortization factor (CAF) is calculated as follows.

$$\text{CAF} = \frac{I}{1-(1+I)^{-20}} \tag{9.14}$$

where, I is the interest rate (taken to be 6% in this calculation). Annual amortization is the product of CAF and CAPEX. This comes to \$4,266.38. In the desalination industry, fixed O & M is often considered to be a maximum of 5% of the CAPEX [74]. The total annual levelized cost is the sum of the annual amortization and annual fixed cost divided by the total amount of water produced in a year. This comes to \$2.30 per cubic meter of water produced. Further, we also assume that the plant is available for only 90% of the time, which is reasonable for thermal desalination systems [74].

Table 9.2 Various components of capital expenditure (CAPEX) for a 10 m^3 per day HDH system.

Component	Cost [$]
Vacuum pumps	1,250.00
Column containers	2,500.00
Pumps	1,600.00
Blowers	2,000.00
Dehumidifier	8,000.00
Humidifier	8,000.00
NG combustor	1,500.00
Generator	1,000.00
Sub contractor costs	15,000.00
Assembly	2,585.00
Controls	5,500.00
Total	48,935.00

Hence, the total cost of water is $4.91 per cubic meter of water produced[4], which is significantly lower than the costs reported for previous HDH systems. Thus, thermal balancing and bubble column dehumidifiers provide substantial improvements to the HDH system which may make them afforable for small scale applications. These applications may include drinking water production in remote settings or remediation of water produced during oil and gas extraction.

Acknowledgments

The authors would like to thank the King Fahd University of Petroleum and Minerals for funding the research reported in this paper through the Center for Clean Water and Clean Energy at MIT and KFUPM (project # R4-CW-08).

[4] This is based on conservative upper limit estimates for CAPEX and is bound to be lower when the advantages of economies of scale are realized.

Nomenclature

Acronyms

CAF	Captial Amortization Factor
GOR	Gained Output Ratio
HCR	Heat Capacity rate Ratio
HDH	Humidification Dehumidification
HE	Heat Exchanger
HME	Heat and Mass Exchanger
RR	Recovery Ratio

Symbols

c_p	specific heat capacity at constant pressure (J/kg.K)
$\dot{H}$	total enthalpy rate (W)
h	specific enthalpy (J/kg)
h^*	specific enthalpy (J/kg dry air)
h_{fg}	specific enthalpy of vaporization (J/kg)
m_r	water-to-air mass flow rate ratio (-)
$\dot{m}$	mass flow rate (kg/s)
N	number of extraction (-)
P	absolute pressure (Pa)
$\dot{Q}$	heat transfer rate (W)
s	specific entropy (J/kg.K)
sal	feed water salinity (g/kg)
$\dot{S}_{gen}$	entropy generation rate (W/K)
T	temperature (°C)

Greek

Δ	difference or change
ε	energy based effectiveness (-)
Ψ	enthalpy pinch (kJ/kg dry air)
Ψ_D	terminal enthalpy pinch (kJ/kg dry air)
η_{tvc}	reversible entrainment efficiency for a TVC (-)

η_e	isentropic efficiency for an expander (-)
φ	relative humidity (-)
ω	absolute humidity (kg water vapor per kg dry air)

Subscripts

a	humid air
c	cold stream
deh	dehumidifier
d	dry air
h	hot stream
hum	humidifier
HE	heat exchanger
in	entering
int	water-vapor interface
max	maximum
local	defined locally
out	leaving
pw	pure water
rev	reversible
w	seawater

Thermodynamic states

a	Seawater entering the dehumidifier
b	Preheated seawater leaving the dehumidifier
c	Seawater entering the humidifier from the brine heater
d	Brine reject leaving the humidifier
e	Moist air entering the dehumidifier
ex	Moist air state at which mass extraction and injection is carried out in single extraction cases
f	Relatively dry air entering the humidifier
g	Air at an arbitary intermediate location in the dehumidifier
i	Seawater at an arbitary intermediate location in the dehumidifier

References

1 Water for people, water for life, executive summary, *Tech. rep.*, The United Nations World Water Development Report (2003).

2 The millennium development goals report, *Tech. rep.*, United Nations, New York, (2008).

3 A. Hammond, The next 4 billion: Market size and business strategy at the base of the pyramid, *Tech. rep.*, Published by World Resource Institute (2007).

4 C. K. Prahalad and A. Hammond, Serving the world's poor profitably, *Har. Bus. Rev.* 4–11 (2002).

5 J. Fawell, K. Bailey, J. Chilton, E. Dahi, L. Fewtrell, and Y. Magara, Fluoride in drinking-water, in *WHO Drinking-water Quality Series, IWA Publishing, London* (2006).

6 B. Bhuyan, A study on arsenic and iron contamination of groundwater in three development blocks of lakhimpur district, assam, india, *Rep. Opin.* **2 (6)**, 82–87 (2010).

7 Appello, Arsenic in ground water a global problem, in *Proceedings of Seminar Utrecht, Netherlands National Committee of IAH*, J. P. Heedreik (2006).

8 A. Annapoorania, A. Murugesan, Ramu, and N. G. Renganathan, Groundwater quality assessment in coastal regions of chennai city, tamil nadu, india – case study, in *Proceedings of India Water Week 2012 - Water, Energy and Food Security*, 10–14, New Delhi, April (2012).

9 H. Strathmann, Ion-Exchange Membrane Separation Processes. *Elsevier*, New York (2004).

10 F. F. Alshare, Investment opportunities in the desalination sector of the kingdom of saudi arabia resulting from privatization and restructuring, in Proceedings of Saudi Water and Power Forum, Jeddah (2008).

11 A. Twort, D. Rathnayaka, and M. Brandt, *Water Supply*. IWA Publishing (2000).

12 G. N. Tiwari, H. N. Singh, and R. Tripathi, Present status of solar distillation, *Solar Energy*, **75(5)**, 367–373 (2003).

13 H. E. S. Fath, Solar distillation: a promising alternative for water provision with free energy, simple technology and a clean environment, *Desalination* **116**, 45–56 (1998).

14 T. A. Lawand, Systems for solar distillation, *Tech. rep.*, Brace Research Institute., Report No. R 115, Sep. (1975).

15 G. P. Narayan, M. H. Sharqawy, E. K. Summers, J. H. Lienhard V, S. M. Zubair, and M. A. Antar, The potential of solar-driven humidification-dehumidification desalination for small-scale decentralized water production, *Renewable and Sustainable Energy Rev.* **14**, 1187–1201 (2010).

16 Y. Li, J. F. Klausner, and R. Mei, Performance characteristics of the diffusion driven desalination process, *Desalination* **196** 188–196 (2006).

17 G. P. Narayan, *Thermal Design of Humidification Dehumidification Systems for Affordable, Small-scale Desalination*. PhD thesis, Massachusetts Institute of Technology (2012).
18 G. Al-Enezi, H. Ettouney, and N. Fawzi, Low temperature humidification dehumidification desalination process, *Energy Conversion Manag.* **47**, 470–484 (2006).
19 B. M. Hamieh, J. R. Beckman, and M. D. Ybarra, Brackish and seawater desalination using a 20 sq. ft. dewvaporation tower, *Desalination* **140**, 217–226 (2001).
20 H. B. Bacha, T. Damak, and M. Bouzguenda, Experimental validation of the distillation module of a desalination station using the smcec principle, *Renewable Energy* **28**, 2335–2354 (2003).
21 H. Müller-Holst, *Solar thermal desalination using the Multiple Effect Humidification (MEH) method in Solar Desalination for the 21st Century*, ch. 15, pp. 215–225. NATO Security through Science Series, Springer, Dordrecht (2007).
22 G. P. Narayan, M. H. Sharqawy, J. H. Lienhard V, and S. M. Zubair, Thermodynamic analysis of humidification dehumidification desalination cycles, *Desalination and Water Treatment* **16**, 339–353 (2010).
23 E. Chafik, A new type of seawater desalination plants using solar energy, *Desalination* **156**, 333–348 (2003).
24 I. Houcine, M. B. Amara, A. Guizani, and M. Maâlej, Pilot plant testing of a new solar desalination process by a multiple-effect-humidification technique, *Desalination* **196**, 105–124 (2006).
25 G. P. Narayan, J. H. Lienhard V, and S. M. Zubair, Entropy generation minimization of combined heat and mass transfer devices, *Int. J. Thermal Sci* **49**, 2057–2066 (2010).
26 G. P. Narayan, K. H. Mistry, M. H. Sharqawy, S. M. Zubair, and J. H. Lienhard V, Energy effectiveness of simultaneous heat and mass exchange devices, *Frontiers in Heat and Mass Transfer* **1**, 1–13 (2010).
27 G. P. Thiel and J. H. Lienhard V, Entropy generation in condensation in the presence of high concentrations of noncondensable gases, *Int. J. Heat Mass Transfer* **55**, 5133–5147~~, May~~ (2012).
28 G. P. Narayan, K. M. Chehayeb, R. K. McGovern, G. P. Thiel, S.M. Zubair, and J. H. Lienhard V, Thermodynamic balancing of the humidification dehumidification desalination system by mass extraction and injection. *Int. J. Heat Mass Transfer* **57(2),** 756–770 (2013).
29 G. P. Narayan, M. S. St. John, S. M. Zubair, and J. H. Lienhard V, "Thermal design of the humidification dehumidification desalination system: an experimental investigation," *Int. J. Heat Mass Transfer* **58**, 740–748 (2013).
30 J. A. Miller and J. H. Lienhard V, "Impact of Extraction on a Humidification-Dehumidification Desalination System," *Desalination* **313**, 87–96 (2013).

31 G. P. Thiel, J. A. Miller, S. M. Zubair, and J. H. Lienhard V, "Effect of mass extractions and injections on the performance of a fixed-size humidification-dehumidification desalination system," *Desalination* **314**, 50–58 (2013).
32. A. Bejan, *Entropy generation minimization: the method of thermodynamic optimization of finite size systems and finite time processes*. Boca Raton, FL: CRC Press (1996).
33 K. H. Mistry, J. H. Lienhard V, and S. M. Zubair, "Effect of Entropy Generation on the Performance of Humidification-Dehumidification Desalination Cycles," *Int. J. Thermal Sci.* **49(9)**, 1837–1847 (2010).
34 S. A. Klein, Engineering Equation Solver, Academic Professional, Version 8, 08 (2009).
35 S. Al-Hallaj, M. M. Farid, and A. R. Tamimi, Solar desalination with humidification-dehumidification cycle: performance of the unit, *Desalination* **120**, 273–280 (1998).
36 S. Soufari, M. Zamen, and M. Amidpour, "Performance optimization of the humidification-dehumidification desalination process using mathematical programming," *Desalination* **237**, 305–317 (2009).
37 M. M. Farid and A. W. Al-Hajaj, "Solar desalination with humidification-dehumidification cycle," *Desalination*, **106**, 427–429 (1996).
38 N. K. Nawayseh, M. M. Farid, S. Al-Hajaj, and A. R.Tamimi, Solar desalination based on humidification process-i evaluating the heat and mass transfer coefficients, *Energy Conversion Manage.* **40**, 1423–1449 (1999).
39 M. Ben Amara, I. Houcine, A. Guizani, and M. Maalej, Experimental study of a multiple-effect humidification solar desalination technique, *Desalination* **170**, 209–221 (2004).
40 C. Yamali and I. Solmus, A solar desalination system using humidification–dehumidification process: experimental study and comparison with the theoretical results, *Desalination* **220**, 538–551 (2008).
41 E. Chafik, Design of plants for solar desalination using the multi-stage heating/humidifying technique, *Desalination* **168**, 55–71 (2004).
42 K. H. Mistry, A. Mitsos, and J. H. Lienhard V, Optimal operating conditions and configurations for humidification-dehumidification desalination cycles, *Int. J. Thermal Sci.* **50**, 779–789 (2011).
43 K. H. Mistry, R. K. McGovern, G. P. Thiel, E. K. Summers, S. M. Zubair, and J.H. Lienhard V, "Entropy generation analysis of desalination technologies," *Entropy* **13(10)**, 1829–1864 (2011).
44 R. K. McGovern, G. P. Thiel, G. P. Narayan, S. M. Zubair, and J. H. Lienhard V. Performance Limits of Single and Dual Stage Humidification Dehumidification Desalination Systems, *Applied Energy* **102**, 1081–1090, Feb. 2013
45 K. M. Chehayeb, G. P. Narayan, S. M. Zubair, and J. H. Lienhard V, "Use of multiple extractions and injections to thermodynamically balance the humidification dehumidification desalination system," *Int. J. Heat Mass Transfer*, ~~accepted, (2013).~~

46 A. P. Colburn and O. A. Hougen, Design of cooler condensers for mixtures of vapors with noncondensing gases, *Ind. Eng. Chem.* **26**, 1178–1182 (1934).
47 W. Nusselt, Die oberflachenkondensation des wasserdampfes, *Zeitschrift des VereinsDeutscherIngenieure* **60**, 541–546 (1916).
48 E. M. Sparrow and E. R. G. Eckert, Effects of superheated vapor and noncondensable gases on laminar film condensation, *AIChE J.* **7**, 473–477 (1961).
49 E. M. Sparrow, W. J. Minkowycz, and M. Saddy, Forced convection condensation in the presence of noncondensables and interfacial resistance, *Int. J. Heat Mass Transfer* **10**, 1829–1845 (1967).
50 W. J. Minkowycz and E. M. Sparrow, Condensation heat transfer in the presence of noncondensables: interfacial resistance, superheating, variable properties, and diffusion, *Int. J. Heat Mass Transfer* **9**, 1125–1144 (1966).
51 V. E. Denny, A. F. Mills, and V. J. Jusionis, Laminar film condensation from a steam-air mixture undergoing forced flow down a vertical surface, *J. Heat Transfer* **93**, 297–304 (1971).
52 V. E. Denny and V. J. Jusionis, Effects of noncondensable gas and forced flow on laminar film condensation, *Int. J. Heat Mass Transfer* **15**, 315–326 (1972).
53 C. Y. Wang and C. J. Tu, Effects of non-condensable gas on laminar film condensation in a vertical tube, *Int. J. Heat Mass Transfer* **31**, 2339–2345 (1988).
54 T. Kageyama, P. F. Peterson, and V. E. Schrock, Diffusion layer modeling for condensation in vertical tubes with noncondensable gases, *Nucl. Eng. Des.* **141**, 289–302 (1993).
55 H. A. Hasanein, *Steam condensation in the presence of noncondensable gases under forced convection conditions*. PhD thesis, Massachusetts Institute of Technology (1994).
56 S. Z. Kuhn, *Investigation of heat transfer from condensing steam-gas mixture and turbulent films flowing downward inside a vertical tubes*. PhD thesis, University of California at Berkeley (1995).
57 N. K. Maheshwari, P. K. Vijayan, and D. Saha, Effects of non-condensable gases on condensation heat transfer, in *Proceedings of 4th RCM on the IAEA CRP on Natural Circulation Phenomena* (2007).
58 H. A. Hasanein, M. S. Kazimi, and M. W. Golay, Forced convection in-tube steam condensation in the presence of noncondensable gases, *Int. J. Heat Mass Transfer* **39**, 2625–2639 (1996).
59 M. Siddique, M. W. Golay, and M. S. Kazimi, Local heat transfer coefficients for forced convection condensation of steam in a vertical tube in the presence of air, *Two-Phase Flow and Heat Transfer (3rd ed.)*, ASME, New York, **197**, 386–402 (1992).
60 V. D. Rao, V. M. Krishna, K. V. Sharma, and P. M. Rao, Convective condensation of vapor in the presence of a non-condensable gas of

high concentration in laminar flow in a vertical pipe, *Int. J. Heat Mass Transfer* **51**, 6090–6101 (2008).
61 B. M. Hamieh and J. R. Beckman, Seawater desalination using dewvaporation technique: experimental and enhancement work with economic analysis, *Desalination* **195**, 14–25 (2006).
62 M. A. Sievers and J. H. Lienhard V, "Design of flat-plate dehumidifiers for humidification dehumidification desalination systems," *Heat Transfer Engrg.* **34(7)**, 543–561 (2013).
63 M. A. Sievers and J. H. Lienhard V, "Design of Plate-Fin Tube Dehumidifiers for Humidification-Dehumidification Desalination Systems," *Heat Transfer Engnrg. accepted* (2014).
64 A. V. Kulkarni and J. B. Joshi, Design and selection of sparger for bubble column reactor. part i: Performance of different spargers, *Chem. Eng. Res. Des.* **89**, 1972–1985 (2011).
65 J. B. Joshi and M. M. Sharma, A circulation cell model for bubble columns, *Chem. Eng. Res. Des.* **57a**, 244–251 (1979).
66 G. P. Narayan, M. H. Sharqawy, S. Lam, and J. H. Lienhard V, Bubble columns for condensation at high concentrations of non-condensable gas: heat transfer model and experiments, *AIChE J.* **59(5)**: 1780–1790, May 2013.
67 E. W. Tow and J. H. Lienhard V, "Analytical Modeling of a Bubble Column Dehumidifier," Proc. ASME 2013 Summer Heat Transfer Conf. HT2013-17763, Minneapolis MN (2013).
68 E. W. Tow and J. H. Lienhard V, "Heat flux and effectiveness in bubble column dehumidifiers for HDH desalination," Proc. IDA World Congress on Desalination and Water Reuse, Tianjin, China (2013).
69 E. W. Tow and J. H. Lienhard V, "Experiments and Modeling of Bubble Column Dehumidifier Performance," *Int. J. Thermal Sci.*, to appear (2014).
70 G. P. Narayan, G. P. Thiel, R. K. McGovern, M. H. Sharaqawy, and J. H. Lienhard V. Vapor mixture condenser. US Patent 8523985 B2.
71 C. Sommariva, *Economics and Financing*. Balaban Desalination Publications (2010).
72 A. K. Plappally and J. H. Lienhard V, Cost of water supply, treatment, end-use, and reclamation, in *Proceedings of European Desalination Society Conference, Barcelona, April 22–26* (2012).
73 J. H. Huang, Design of a mobile community level water treatment system based on humidication dehumidication desalination. SB Thesis, Massachusetts Institute of Technology, June (2012).
74 US Energy Information Administration. URL: http://www.eia.gov/countries/cab.cfm?fips=IN. 2012.